Environmental Modelling & Software 49 (2013) 1–21

Contents lists available at ScienceDirect

Environmental Modelling & Software

journal homepage: www.elsevier.com/locate/envsoft

Integrated assessment model of society-biosphere-climate-economy-energy system

Mohammad K. Akhtar [a,*], Jacob Wibe [b], Slobodan P. Simonovic [c], Jim MacGee [d]

[a] Authorization, Ministry of Forests, Lands and Natural Resource Operations, Surrey, British Columbia, Canada
[b] Department of Economics, University of Colorado, Denver, CO, USA
[c] Department of Civil and Environmental Engineering, The University of Western Ontario, London, Ontario, Canada
[d] Department of Economics, The University of Western Ontario, London, Ontario, Canada

ARTICLE INFO

Article history:
Received 9 March 2013
Received in revised form
10 July 2013
Accepted 12 July 2013
Available online

Keywords:
System dynamics simulation
Feedback
Climate change
Integrated assessment modeling
Society-biosphere-climate-economy-energy system
Optimization

ABSTRACT

The feedback based integrated assessment model ANEMI_2 represents the society-biosphere-climate-economy-energy system of the earth and biosphere. The ANEMI_2 model is based on the system dynamics simulation approach that (a) allows for the understanding and modeling of complex global change and (b) assists in the investigation of possible policy options for mitigating, and/or adapting to changing global conditions within an integrated assessment modeling framework. This paper outlines the ANEMI_2 model and its nine system components: climate, carbon cycle, land-use, population, food production, hydrologic cycle, water demand, water quality, and energy-economy. To evaluate market and nonmarket costs and benefits of climate change, the ANEMI_2 model integrates an economic optimization approach, with a focus on the international energy stock and fuel price, climate interrelations and temperature change. The model takes into account all major greenhouse gases (GHG) influencing global temperature and sea-level variation. Results from several scenarios (a) compare well with other information available in the scientific literature, (b) present comprehensive response of the society-biosphere-climate-economy-energy system to the selected scenarios, and (c) confirm the support role of the ANEMI_2 model in the policy development and analyses.

Software availability

The ANEMI model code and data used in this study are available in Akhtar (2011). The model is available for further research use upon request (simonovic@uwo.ca).

1. Introduction

The earth's climates have changed in the past and will change in the future. Climate change has been a subject of research interest for many years and the attention has been growing with the awareness of relationship between climate change and socio-economic dynamics. Although there exists considerable knowledge of the broad characteristics of the climate, there is still need for improved understanding of how the major processes of climate change – of the world's oceans, ice masses, exposed land surface and socio-economic processes – interact.

Integrated assessment modeling, supported by the improvement of computer technology, surfaced in the mid-1980s as a new paradigm for interfacing science and policy concerning complex environmental issues such as climate change. According to Parson (1994): "To make rational, informed social decisions on such complex, long-term, uncertain issues as global climate change, the capacity to integrate, reconcile, organize, and communicate knowledge across domains – to do integrated assessment – is essential." Therefore, integrated assessment models are believed to produce insights that cannot be easily derived from the individual natural or social science component models that have been developed in the past (Laniak et al., 2013; Weyant, 1994).

ANEMI modeling effort at the University of Western Ontario, Canada uses a system dynamics simulation approach for integrated assessment of climate change impacts (Davies and Simonovic, 2010, 2011). The ANEMI_2[1] model, presented in this paper, represents the society-biosphere-climate-economy-energy system on a global scale (Akhtar, 2011; Akhtar et al., 2011). To evaluate market and nonmarket

* Corresponding author. Water Allocation, Ministry of Forests, Lands and Natural Resources Operations, Suite 200, 10428-153 Street, Surrey, British Columbia V3R 1E1, Canada. Tel.: +1 604 497 1632.
E-mail address: khalediwm@yahoo.com (M.K. Akhtar).

[1] ANEMI_2 is an integrated assessment model consisting of nine system components: climate, carbon cycle, energy-economy, land-use, food production, population, hydrologic cycle, water demand, and water quality.

1364-8152/$ – see front matter © 2013 Elsevier Ltd. All rights reserved.
http://dx.doi.org/10.1016/j.envsoft.2013.07.006

costs and benefits of climate change, the ANEMI_2 model integrates an economic approach, with a focus on the international energy stock and fuel price, with climate interrelations and temperature change. The model takes into account all major greenhouse gases (GHG) influencing global temperature and sea-level variation. Several of the model system components are build upon the basic structure of the ANEMI_1 model developed by Davies (2007). The ANEMI_2 model extends the system dynamics simulation approach by integrating it with an optimization algorithm capable of describing the energy-based economic activities that affect long-term Earth-system behavior. Experimentation with different policy scenarios demonstrates the consequences of these activities on future behavior of the society-biosphere-climate-economy-energy system through feedback based interactions. The use of the ANEMI_2 model improves both, the scientific understanding of the complex global system and the socio-economic policy development (Akhtar, 2011). This paper describes the ANEMI_2 model structure in detail and illustrates its use through the analyses of three global policy scenarios.

Section 2 of the paper summarizes the different modeling approaches used in the development of ANEMI_2 model. The following section (Section 3) provides a brief description of the model's individual system components. Section 4 describes the experimentation undertaken to analyze three policy scenario associated with water resources use, carbon tax introduction, and change in land use. Section 5 summarizes and evaluates the significant results of model simulations against research objectives. The paper ends with recommendations for future research.

2. Model of the society-biosphere-climate-economy-energy system

> *"Climate change is expected to exacerbate current stresses on water resources.[…] Widespread mass losses from glaciers and reductions in snow cover over recent decades are projected to accelerate through the 21st century, reducing water availability, hydropower potential, and changing seasonality of flows [in some regions]."*
>
> Intergovernmental Panel on Climate Change, (2007a).

Climate system modeling with General Climate Models (GCMs) is currently the best choice for analyzing the physical climate system. However, the climate system modeling has been evolving towards Earth system modeling by considering dynamics and complexity of atmosphere, oceans, land surface, and biosphere (Jacobson et al., 2008). In spite of this scope, the earth system modeling abstracts from socio-economic forces, which are the main driving forces behind rapid climate change. Therefore the integrated assessment modeling (IAM) provides a convenient framework for combining knowledge from a wide range of disciplines.

Climate change economics are largely developed using the general equilibrium theory of Arrow and Debreu (Shafer and Sonnenschein, 1975). This approach utilizes optimization methods to characterize the supply and demand functions for energy and system components output. The other model system components use system dynamics based simulation that allows a very detailed mathematical representation of each component, such as WaterGAP2 (Alcomo et al., 2003). Hence integration of optimization and system dynamics simulation is carried out under the integrated assessment modeling framework in the development of ANEMI_2 model (Akhtar, 2011).

2.1. Integrated assessment modeling

IAMs available today (DICE, AIM, MERGE, ICAM, FREE, MESSAGE, IMAGE and so on) are used in (i) policy optimization (such as DICE, which seeks optimal policy strategies) and (ii) policy evaluation (such as IMAGE, which assesses specific policies). Optimization models are normative in character and typically analyze climate change from an economic perspective, i.e., they focus on the efficiency and rationality of a policy (Tol and Fankhauser, 1998). The level of optimization modeling details makes the optimization algorithm unmanageable. Due to computational limitations, optimization models tend to be based on compact representations (high degree of generalization) of both the socio-economic and natural science system components. They thus contain a relatively small number of equations, with a limited geographic coverage. Policy evaluation models tend to be descriptive and contain much more details describing physical, economic and/or social system components. These models are often referred to as simulation models, and are designed to calculate the consequences of specific climate policy strategies in terms of a suite of environmental, economic, and social performance measures.

Over the past decade or so, IAMs have been widely utilized to analyze the interactions between human activities and the global climate (Laniak et al., 2013; Weyant et al., 1996). They are usually comprehensive, but produce less detailed models than the conventional climate- or socio-economic-centred modeling. As Rotmans et al. (1997b: 36) note, IAMs "are meant to frame issues and provide a context for debate. They analyze problems from a broad, synoptic perspective." It is a system-wide approach, where one tries to look at various components of a system as a whole. However, it is always an issue to sacrifice between representing depth in individual system components and representing breadth of the overall system (Kelly et al., 2013). Therefore the challenge to integrated assessment modeling is to capture the sufficient depth of individual system components without compromising breadth of the overall system.

The first IPCC report referenced two IAMs, the Atmospheric Stabilization Framework developed by the US Environmental Protection Agency (EPA) and the Integrated Model for the Assessment of the Greenhouse Effect (IMAGE) model (Rotmans, 1990; Van Vuuren et al., 2006). These were employed to assess the factors controlling the emissions and concentrations of GHGs over the next century. The MAGICC model was subsequently developed to incorporate ocean heat transport and a carbon cycle component to capture land-use change (Meinshausen et al., 2008). A regional Integrated Assessment Tool (RIAT) is recently developed by Carnevale et al. (2012) to assess air quality. It implements a multi-objective problem for the selection of effective policies to control pollution exposure to primary and secondary pollutants. Davies (2007) provides some examples of integrated assessment models including the Integrated Model to Assess the Greenhouse Effect, IMAGE 2.0 (Alcamo, 1994), the Asian Pacific Integrated Model, AIM (Matsuoka et al., 1995), the Model for Evaluating Regional and Global Effects of GHG reduction policies, MERGE (Manne et al., 1995), the Tool to Assess Regional and Global Environmental and health Targets for Sustainability, TARGETS (Rotmans and de Vries, 1997), the Integrated Global System Model, IGSM (Prinn et al., 1999), Integrated Climate Assessment Model, ICAM (Dowlatabadi, 2000), the Dynamics Integrated Climate-Economy model, DICE (Nordhaus and Boyer, 2000), the Feedback-Rich Energy-Economy model, FREE (Fiddaman, 1997, 2002), and World3 (Meadows et al., 2004). Because of their significant flexibility the IAMs are also been extensively used for agricultural system policy impact assessment to climate change (Bland, 1990; Van Ittersum et al., 2008; Ewert et al., 2009; Lehtonen et al., 2010).

Following the development path of IAMs, a circular references or "feedbacks" based model ANEMI_1 was introduced in 2007 and underwent a moderate modification in 2009 with the addition of energy system component (Davies, 2007; Davies and Simonovic, 2008, 2010). However, a relatively simple representation of the macro-economic system of the ANEMI_1 model is limiting accurate simulation of change in primary and secondary energy supply and demand. In short, the ANEMI_1 is not able to project reasonable industrial emission paths. To overcome these problems, an integrated economic optimization approach is introduced within the system dynamics simulation environment and named ANEMI_2 model.

2.2. System dynamics simulation

System dynamics simulation (SD) approach, in the current form, originates from the pioneering work of Forrester (1958) in the field of business management at the Massachusetts Institute of Technology (MIT), Cambridge. Today, the system dynamics simulation is used in various disciplines of natural, social and health sciences. The SD modeling tools were originally developed with the intention of facilitating the interplay between the manager's mental models and the analyst's formal models. With time, the system dynamics modeling has become a prominent tool in the area of public policy. Much of the art of system dynamics modeling is in discovering and representing the feedback processes, with stock and flow structures, time delays, and nonlinearities to help determine the dynamics of a system (Sterman, 2000).

Over the last 50 years, system dynamics applications in Water Resource Management (WRM) have branched off in many directions. Simonovic (2009) and Winz et al. (2009) categorized these by their main problem focus: regional analysis and river basin planning, urban water management, flooding, irrigation and pure process models. Thus, the system dynamics models help to inform decision-making.

A number of projections of future CO_2 emissions from energy use have used linear models without explicit description of feedback mechanisms. SD models offer an opportunity for assessing the quantitative importance of feedbacks on system dynamics. The Carbon Bathtub of Sterman is an extremely basic example of the Earth's growing CO_2 emissions (Kunzig, 2009). The system dynamics simulation models integrate knowledge from different disciplines using a single platform. The following are some examples: DICE – Dynamic Integrated model of Climate and the Economy (Nordhaus, 1994); RICE – Regional Integrated model of Climate and the Economy (Nordhaus and Yang, 1996); FREE (Fiddaman, 1997); and ANEMI_1 (Davies and Simonovic, 2008, 2009). All these models contain the traditional energy-economy system component on one side and the Earth system model that incorporates the climate system component on the other.

2.3. Integrated optimization-simulation modelling

Simulation models describe how a system operates, and are used to predict what changes will result from a specific course of action (Simonovic, 2009). The simulation predicts the outcome of a single set of design and/or policy variables. Simulation gives one solution for one set of inputs and another solution to another set of inputs. Selecting various input options (simulations scenarios) allows deeper insight into system behavior. Optimization models are useful for screening alternatives and reducing the number that needs to be simulated in detail. Optimization algorithms are efficient in searching feasible policy space and identifying an optimal policy choice according to the given objective/s and set of constraints. Optimization models are thus generally used for the preliminary evaluation or screening of alternatives. They thus identify important data needs prior to extensive data collection and simulation modeling activities (McKinney and Savitsky, 2003). The objective of any optimization process is to coordinate the simulation of a sequence of system configurations, where each configuration corresponds to a particular choice of decision variables. Therefore, a system configuration is ultimately obtained that provides an optimal or near optimal solution (Law and McComas, 2000).

Until the end of the last millennium, optimization and system dynamics simulation were kept largely separate. Kasperska et al. (2000, 2001) embedded optimization procedures in their system dynamics simulation models, while optimizing the dynamics balance of a production process. They dealt with two methods of embedding optimization procedures in the SD simulation models. The first way they undertook the problem was in relation to Legras's idea regarding the so-called "pseudosolution" of equation: $Ax - b = 0$, *which minimizes the norm of these differences*. Here, b is a vector of a known coefficient, x represents the vector of decision variables, and A is a (known) coefficient matrix. In the second way they took advantage of the Linear Programming optimization. They called this approach "embedding linear programming in System Dynamics" (Kasperska and Slota, 2003).

The available literature indicates that simulation based optimization has been used primarily in computer and chemical engineering for supply chain management (Truong and Azadivar, 2003; Hung et al., 2004; Erdem and Sancarin, 2006; Almeder and Margaretha, 2007; Amodeo et al., 2009). However, side by side simulation based optimization techniques have also attracted water resources management researchers (Bhattacharjya and Datta, 2005; Fedra and Harmancioglu, 2005; Pulido-Velazquez et al., 2006; Cetinkaya et al., 2008; Safavi et al., 2010; Bashi-Azghadi and Kerachian, 2010; Singh, 2011). Apart from these, such approaches have also been well accepted in other computational arenas, such as risk management (Better et al., 2008) and fishery management (Azadivar et al., 2002).

The (few) optimization based simulation models in the field of integrated assessment modeling include MERGE (Manne et al., 1995), REMIND (Luderer et al., 2009; Leimbach et al., 2010), and MiniCAM (Calvin et al., 2009). MERGE solves in each period for the optimal emission prices that meet a long-term target. At each point in time, supply and demand are equilibrated through the price of internationally traded commodities: oil, gas, coal, carbon emissions rights and a numeraire good (composite of all items produced outside the energy system component). REMIND is a global energy-economy-climate model that builds on the neoclassical growth model, and solves for inter-temporal global welfare subject to equilibrium constraints. MiniCAM is a recursive partial equilibrium model with a long-term time horizon that runs in 15-year time steps. In the MiniCAM model, the focus is on energy and agriculture, i.e. the clearing of energy and agricultural goods. The mechanism for clearing the markets is part of the solution algorithm, which adjusts market prices awaiting the excess demand. The deviation between demand and supply needs to be smaller than the suggested criteria, which is typically a small number.

The ANEMI_2 model differs from these IAMs in how it merges a system dynamics approach with a neo-classical growth model. The non-linear nature of the energy-economy system component in the ANEMI_2 model requires the solution of a nonlinear system of equations. We have utilized the trust-region method (Conn et al., 2000) with dogleg algorithm to solve this system. As these models have a significant number of nonlinear equations to solve, the Gauss–Newton method with a line search is not a robust choice. Because of its unique system dynamics based feedback structure, the ANEMI_2 model is solving – an optimal allocation problem within each simulation time step (such that optimization is carried out based on the current state of the system without considering future projections). Thus, unlike other integrated assessment models which take as an input the resource paths, the

ANEMI_2 model generates an endogenous path for energy supply. For example, the MERGE has more detailed energy system component compared to the available IAMs. It takes into account different fossil fuel energy sources while computing the energy price. But in calculating the energy price, the ANEMI_2 takes into account not only known fossil fuel energy reserves; it also takes into account probable energy discoveries (for each type of fossil fuel), availability of hydro and nuclear energy, and technological changes.

The ANEMI_2 model tackles several key shortcomings of the ANEMI_1 model. The ANEMI_1 model assumed an exogenous approach to investment in electricity generation, and as a result total investment is dynamic only in the sense that it meets the demand, which rises over time through economic development. Because of its simulation based structure, the energy demand is also represented in a simple fashion that does not adequately capture historical changes in behavior. The economic output of ANEMI_1 is not tied to energy demand or price, and this leads to the dramatic fluctuation of energy prices without affecting the economic system. The ANEMI_2 model involves an optimal allocation of investment across different energy sources each period, so that the optimization routine is integrated in the energy-economy system component.

3. ANEMI_2 model description

The ANEMI_2 model combines nine system components interlinked through multiple feedbacks in order to capture the complexity of the socio-economic-climate system. The model reproduces the structure of the socio-economic-climate system (through the selection of system elements and their relationships) rather than simulating system behavior using the traditional process of matching simulated and observed model behavior. The structural approach allows for a more scientific representation of the feedback relationships and simulation of system behavior caused by system structure.

ANEMI_2 represents each system component either in zero-dimensional or one-dimensional form. Here, dimensionality refers to the degree of aggregation within a system component. Zero-dimensional system components model important characteristics and processes at a *global-aggregate level*, while one-dimensional system components have *one spatial dimension*. The ANEMI_2 consists of nine system components: climate, carbon cycle, energy-economy, land-use, food production, population, hydrologic cycle, water demand, and water quality (Akhtar, 2011). These system components are of varying complexity. The land-use and population system components are relatively simple, while the carbon cycle and water-related system components have a more complex structure. Fig. 1 shows the structure of the ANEMI_2 model, with system component names in bold. The arrows connect the individual system components with the use of influencing variables (in italics). The direction of the arrow indicates the information flow direction between the system components, while positive and negative signs indicate direction of change in connected system components (positive sign indicates the increasing/decreasing change in both connected system components while the negative sign indicates the change in opposite direction between the connected system components). The subsequent sections provide detailed description of each system component.

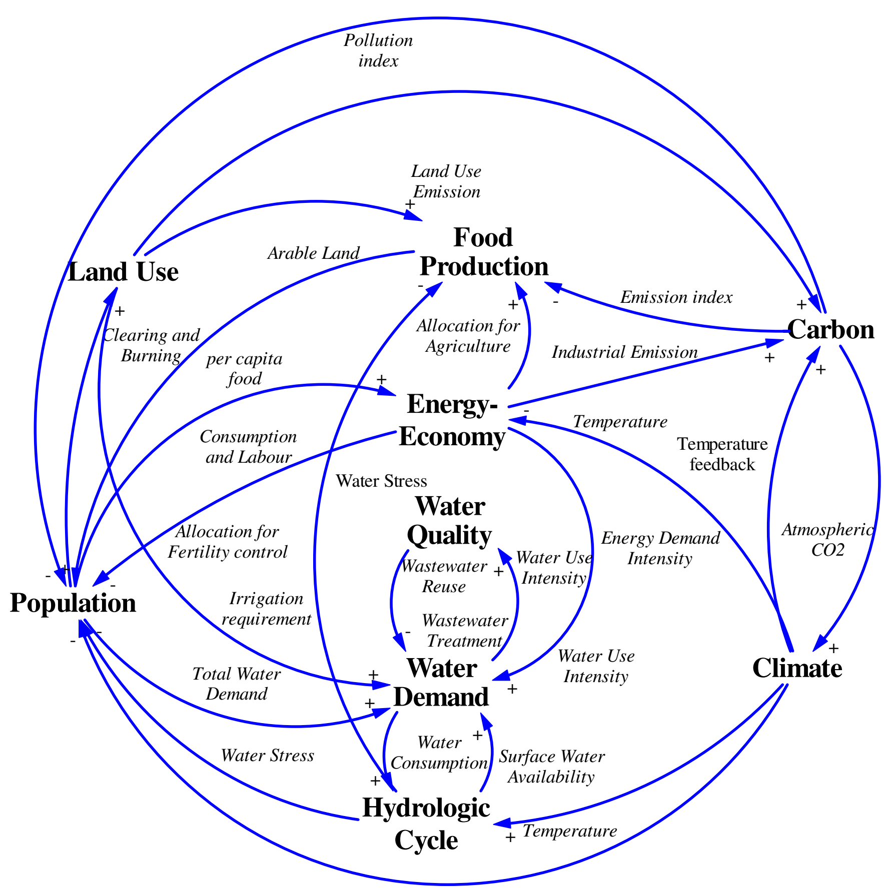

Fig. 1. Causal-loop diagram of the ANEMI_2 model (after Akhtar, 2011).

3.1. Population system component

Two basic dynamics of the society-biosphere-climate-economy-energy system of the Earth are a) the tendency of human population towards exponential growth, and b) the long delay in the adaptive response of a population to changing external conditions (Meadows et al., 1974, 1992). The actual rate of growth, the nature of the adaptive response, and the length of delay all vary, depending on many different factors. It's worthwhile to mention that even though the basic structure of the population system component of the ANEMI_2 model is adopted from WORLD3 model, the parameters are adjusted separately (before combining these nine system components all together) to be as close as possible to the historical observations.

When any biological population grows, the pattern of growth over time tends to be exponential. The total increase in the global population during any time period is determined at least partially by the size of the population of reproductive age in that time period. The population system component of ANEMI_2 includes a four-level population model. The population is divided into 4 age groups (0–14 yr; 15–44 yr; 45–64 yr; and 65 plus yr). The schematic of the population system component is shown in Fig. 2.

The population system component of the ANEMI_2 model is based on the WORLD3 population model (Meadows et al., 1974, 1992). It represents continuous dynamic interactions among the human population, climate and global resources. The population system component model contains numerous feedback loops representing demographic and technological-economic means of achieving a favorable balance between the population size and the supply of resources. In the ANEMI_2 model crowding, pollution, availability of food, and household income affect average life expectancy. Therefore, life expectancy is a dynamic variable which changes with the change of its associated components over time. Life expectancy and extreme temperature determine the population death rate. Fertility is determined by a number of factors, including fertility control effectiveness, capital allocation, and desired family size. Birth and death rates are the only two direct variables used in the population computation.

Four factors: (i) food, (ii) health services, (iii) crowding, and (iv) pollution are incorporated in the equation for life expectancy as modifiers, or multipliers, of a 'normal' life expectancy. The normal life expectancy can be set at any arbitrary value as long as the four multipliers are all defined properly with respect to that value.

$$L_E = L_{EN} \cdot L_{MF} \cdot L_{MHS} \cdot L_{MP} \cdot L_{MC} \tag{1}$$

where L_E is the life expectancy, L_{EN} is the life expectancy normal, and L_{MF} is the lifetime multiplier from food. Lifetime multiplier from health service, persistent pollution, and crowding are respectively represented as L_{MHS}, L_{MP}, and L_{MC}.

In the population system component the number of deaths per year (D_{er}) is expressed as the total number of people of a specific age group (P_{agr}) multiplied by the mortality (P_{mor}) of the same group.

$$D_{er} = P_{agr} \cdot P_{mor} \tag{2}$$

where mortality is a function of life expectancy. This functional relationship is expressed in Meadows et al. (1974, page 170–172) as:

$$P_{mor} = f(L_E) \tag{3}$$

Thermal stress related mortality should increase due to global warming. For human populations, 16°–30 °C is the comfortable temperature zone. In some studies, population over 60 years of age is found to be at highest risk (Applegate et al., 1981; Macfarlane, 1978), while other investigators report the highest-risk age groups to be those over 65 years of age (Macfarlane, 1978; Jones et al., 1992; Saez et al., 1995; Wainwright et al., 1999; Smoyer-Tomic and Rainham, 2001), 70 years of age (Ellis et al., 1980; Ballester et al., 1997). However, other heat-wave studies report no differences between males and females or between Whites and non-Whites (Ellis and Nelson, 1978). Thus, heat-related mortality primarily affects the elderly, infants, and people of lower socio-economic status. The evidence for influences of race and gender has been inconsistent (Basu and Samet, 2002). Children under 15 years (O'Neill et al., 2005; Gouveia et al., 2003), children five years and younger (Basu and Ostro, 2008), and infants one year of age and under (Basu and Ostro, 2008; Diaz et al., 2006) have been identified to be at high risk of mortality from extreme temperature (Basu, 2009). A comparative study is carried out by El-Zein and Mylene (2005) to establish a relationship between the high temperature and mortality in warm climates. Nichollas (2009) also investigates changes in mortality due to climate change. However, most of the references are focused on high temperature and lag time while considering extreme daily temperature. Martens (1998) finds that death rate increases 1% with each 1-degree Celsius drop in temperature below 16° and 1.4% per degree rise above 30 °C. Martens'

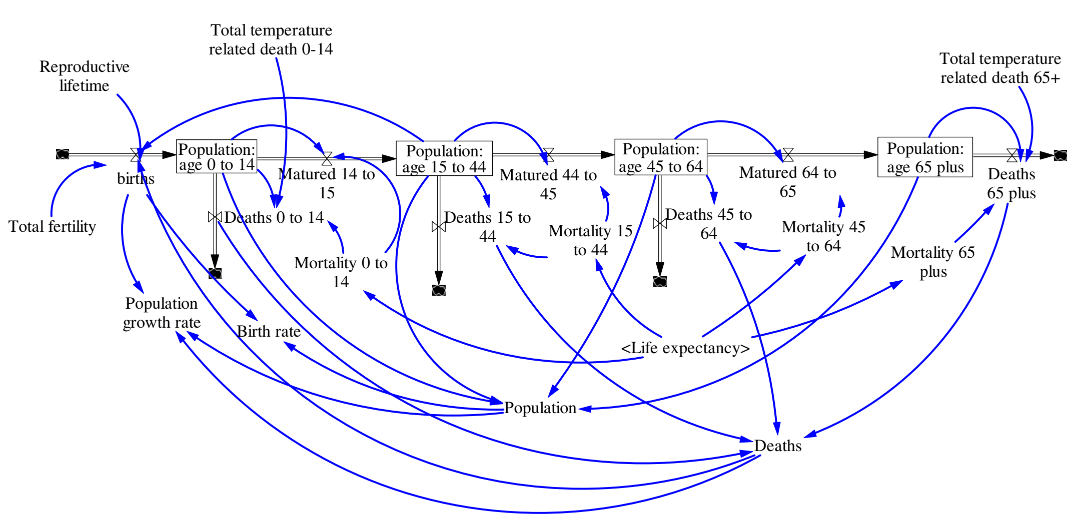

Fig. 2. Model structure of the ANEMI_2 population system component.

findings are implemented in our model. Since children and elderly (population above 65 years of age) are most vulnerable to extreme temperatures, heat related death is incorporated in the ANEMI_2 model for two age categories (0–14 and 65 plus). Equation (2) changes as follows for these two age groups:

$$D_{er} = P_{agr} \cdot P_{mor} + D_{heat} \tag{4}$$

The number of births per year (B_{er}) is calculated using the number of fertile women in the population (half of the total population between the 15 and 44 age group), and the average number of births per women per year.

$$B_{er} = F_{total} \cdot \frac{0.5 \cdot P_{15-44}}{R_{life}} \tag{5}$$

where F_{total} is the total fertility, R_{life} is the reproductive lifetime of 30 years, and P_{15-44} is the total population between age 15 and 44.

Total fertility is computed from the maximum total fertility (F_{Mtotal}), desired total fertility (F_{Dtotal}) and fertility control effectiveness (F_{econt}):

$$F_{total} = \mathrm{MIN}(F_{Mtotal}, \; F_{Mtotal} \cdot (1 - F_{econt}) + F_{econt} + F_{Dtotal}) \tag{6}$$

3.2. Food production system component

The global amount of food that can be produced each year is limited by available resources. Even with the limited resources food production can be enhanced with proper allocation of physical resources (water, fertilizer, suitable land, etc.) along with technological innovations. Though it has become evident that there are decreasing returns to technology's ability to increase the land yield by diverting the input of other limited resources into the agriculture system component (Meadows et al., 1974; Postel, 1999). The complex land yield is obtained from the variables of land fertility, water-stress, and capital investment. The total amount of food produced depends on factors like land yield, availability of the agricultural land, availability of the water for irrigation, and etc.

Arable, cultivated land is at present the most important source of food production for human consumption. But it is not the only one. Other sources of food production include the oceans and the world's grazing lands. However, FAO data (AQUASTAT, 2010) shows that only 7.4% of the total amount of food product comes from animal products. In the last few decades the world has seen a noticeable shift in food consumption patterns towards more animal products such as meat, milk and eggs, mainly due to growing economies and rising individual income, especially in developing countries. However, on a global scale such rise is not so dramatic. It is assumed that the crop production needs to be increased by 66% and animal production by 85% (compared to 2007) to meet the rising demand in 2050 (Bruinsma, 2009). Even with such higher increase of animal product will not be able to change the ratio between crop and animal product consumption significantly. It is recommended that future model expansion consider addition of the animal sub-component under Food Production system component, even though the net animal product consumption is not expected to rise rapidly on the global scale (Kearney, 2010).

The current and potential food output from both fisheries and grazing land is thus small compared to the food output from the cultivation of arable land. Therefore, the ANEMI_2 model abstracts from the food obtained from oceans and grazing lands. The average carrying capacity (the number of animals that can be placed on a pasture or rangeland for an entire season without harming it) of the world's grazing lands is roughly 1 animal unit per 12 ha, where 1 animal unit is equivalent to the production of 100 kg of meat per year (Meadows et al., 1974; Stanley, 2009). However, it's very difficult to come up with a single value because the carrying capacity depends on many factors: type of cattle, type of grass, soil type, and median rainfall. Even in the ILRI report the carrying capacity is different in each region (Watson and van Binsbergen, 2008). If it is assumed that 7 kg of vegetable crops are needed to produce 1 kg of meat, this yields the amount of 35 vegetable-equivalent kilograms per hectare per year. Thus the vegetable-equivalent food yield from grazing lands is low in comparison to the traditional yield of 600 vegetable-equivalent kilograms per hectare-year that can typically be obtained from arable land without the use of modern agricultural inputs.

The food production system component (Fig. 3) of the ANEMI_2 model is adopted from WORLD3 model (Meadows et al., 1974, 1992). In this model, the capital investments in agriculture can increase total food production in two ways: (a) by increasing the stock of arable land through land development, and (b) by increasing land yield through application of material inputs (pesticides, seed, feed, fuel, electricity, rented machinery, repairs, miscellaneous inputs, and three types of fertilizer).

The agriculture system component also distinguishes between two phenomena that can reduce overall food production. The first one is 'land erosion': an irreversible centuries-long process that physically removes land from production. The rate at which land erodes can be large or small, depending on the human actions taken to control the erosion rate. The second phenomenon that can reduce land yield, and thus food production, is 'lower land fertility',

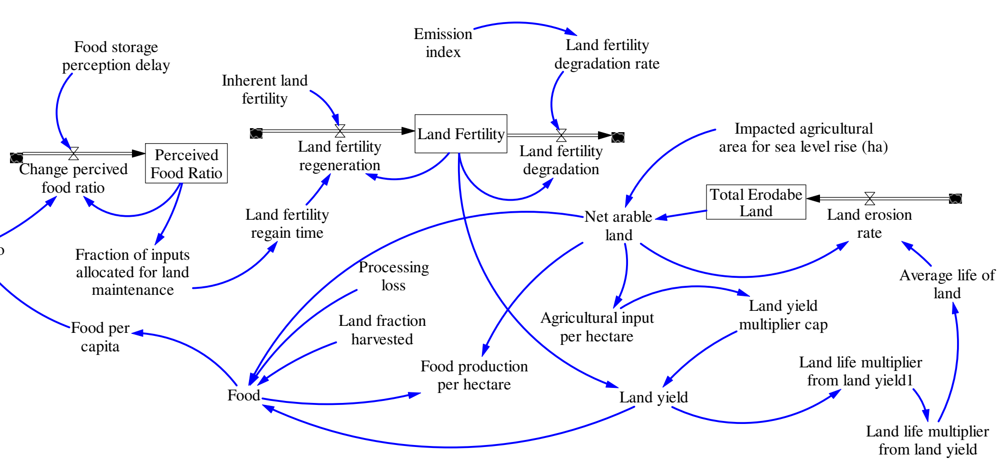

Fig. 3. Model structure of the ANEMI_2 food production system component.

that is, by a reduction in the humus and nutrient content of the soil. This is a reversible process, since the degradation of the land's fertility occurs only when insufficient resources are allocated to the enhancement of the natural soil's regeneration mechanisms.

In the ANEMI_2 model all types of arable land are included in a single stock, so the model reflects in a single quantity, the aggregate of all different lands with the varying cultivation characteristics.

Technological change affects relationships in the agriculture system component in a variety of ways. Some of the effects of advances in technological capability are included endogenously in the food production system component. It is assumed (for simplicity) that the allocation of more investment to increase in land yield will result in roughly the same average return on a global scale. It is acknowledged that the return will differ on a regional scale.

The complex land yield is obtained from the variables of land fertility (average crop output per hectare of net arable land), water-stress and capital investment. Water scarcity is often measured by water stress, defined as "a measure of the degree of pressure put on water resources by users of the resources, including municipalities, industries, power plants and agricultural users" (Alcamo and Henrichs, 2002). The most common water stress indicator is the "annual withdrawals-to-availability (wta)" ratio, where wta values of 0.2 indicate "mid-stress" and values of 0.4 and higher indicate "severe stress". All of these variables are connected with positive polarity (the increase/decrease in one causes the increase/decrease of other). The total amount of food produced depends on such factors as land yield, availability of the agricultural land, availability of the water for irrigation, and so on. In ANEMI_2 model, the food ratio works like a thermostat, by which extra investment is pumped in the food production system component, when the ratio is below the threshold level. The extra investment is used to improve land fertility, while technological development is used to enhance the food production by increasing the land yield.

Total annual food production in ANEMI_2 is a function of cultivated land and land yield. This specification implicitly assumes that there is no shortage of labor force, which is why we did not consider labor hours in our model. Thus the food output is calculated simply as the output per hectare of harvested land times the total cultivated land area.

$$F_p = L_y \cdot A_l \cdot L_{fh} \cdot (1 - P_l) \tag{7}$$

where F_p is the amount of food production, L_y is the land yield. The net arable land, land fraction under harvesting, and processing loss are denoted by A_l, L_{fh} and P_l respectively. The land yield L_y is the average total weight of crop production on a hectare of land per year. In the ANEMI_2 model land yield is partly computed by land fertility, defined as the weight of crop that land will produce using only traditional inputs, such as human or animal energy, and natural fertilizers, such as manure. The land yield L_y, can be increased significantly above the land fertility by the use of modern agricultural inputs.

$$L_y = L_{yf} \cdot L_{fert} \cdot L_{ymc} \cdot L_{ymw} \tag{8}$$

where L_{yf} is the land yield factor, L_{fert} is the land fertility, and L_{ymc} is the land yield multiplier from capital. Availability of water resources is a vital component of the land yield, therefore Equation (8) also introduces water-stress into calculation of land yield factor (L_{ymw}).

Land fertility (L_{fert}) is the average crop output per hectare of net arable land (A_l) without the use of modern agricultural inputs. The fertility of the land is a complex function of the organic and inorganic content of the soil, the climate, and the incident solar radiation. Any process that interferes with soil chemistry, or the water holding capacity of the soil, is likely to change soil fertility. There are many such processes, some with positive influence tending to regenerate soil fertility and some tending to degrade it. A simple way of formalizing land fertility, where L_{fr} and L_{fd} stand for land fertility regeneration and land fertility degradation respectively is shown below. Land fertility regeneration is describing ability of soil to provide all of the nutrients required by the crop. The availability of nutrients is normally greater when they are associated with organic matter. Soil chemical fertility can be enhanced by applying manure, fertilizer, compost and lime. Soil fertility degradation is triggered by nutrient removal through plant uptake, erosion and leaching, described as soil mining. In addition, soil degradation can be increased due to the impacts of climate change (wildfires, floods, droughts, wind/dust storms, solar radiation and so on).

$$L_{fert} = \int \left(L_{fr} - L_{fd}\right) \cdot dt \tag{9}$$

The calculation of net arable land (A_l) combines different inputs, including impacted agricultural land due to sea-level rise. It represents the net cultivated area that is dedicated directly to human food production. Therefore, it excludes the land area used for the production of fodder and animal crop (L_{fa}), and can be expressed as:

$$A_l = (L_{ar} - L_{ero}) \cdot L_{obs} - L_{slr} - L_{fa} \tag{10}$$

where L_{ar} and L_{ero} respectively represent arable land and net erodible land. An obstacle to land conversion is defined as L_{obs} and impacted agricultural land is denoted as L_{slr}.

3.3. Energy-economy system component

The energy-economy system component in the ANEMI_2 model describes the world's energy resources, and how prices move to balance the global demand and supply of energy. The energy-economy extends the (Solow) neoclassical growth model to incorporate an energy system component. The novel part of ANEMI_2 is the allocation of energy production across fossil fuels, hydro, nuclear, and alternative energy sources.

The model follows common practice in macroeconomics in assuming the global economy is populated by a representative household and firm. The household has preferences over an aggregate consumption good and supplies labor services inelastically to the firm in each period. The firm takes labor, capital, and energy services as inputs in a Cobb-Douglas production function, and produces the final good which is used for consumption and investment. Investment in capital each period is equal to a fraction s of output. There is no trade in the model.

Aggregate 'Energy services' is modeled as a composite good produced using heat energy and electric energy. Heat energy is produced from fossil fuels and alternative energy sources. Electric energy is produced from fossil fuels, nuclear, and hydro power.

The production of output is negatively affected by climate change (climate damages). The global mean temperature represents a negative feedback to the economic system from industrial emissions through climate damages (Fig. 4).

3.3.1. The representative household

The world's population is represented by a stand-in household whose preferences can be represented by the utility function

$$U(C) = \ln(C) \tag{11}$$

where C is the final consumption good. The household supplies labor, L, inelastically to the market. We assume that the household owns the world's capital stock and natural resources. Thus, the consumer rents the capital to the firm, earning income rK, where r

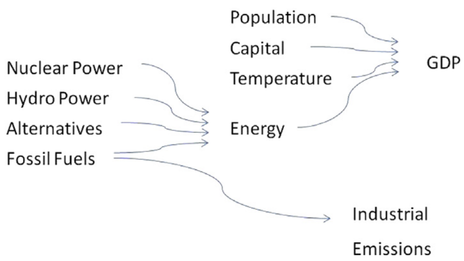

Fig. 4. Causal loop diagram of ANEMI_2 energy-economy system component.

is the interest rate and K is the aggregate capital stock in the economy. The consumer also sells energy services to the firm, earning income $P_E E$, where E is aggregate energy services, and P_E is the price of aggregate energy services.

Investment, I, is assumed to follow a Solow investment rule where a fraction s of output, Y, is invested into new capital each period. The household budget constraint in each period is:

$$rK + wL + P_E E - \overline{T} \geq C + I \tag{12}$$

$$I = sY$$

$$T = \sum_i \tau_i F_i$$

where T is total tax revenue which is rebated lump-sum to the household.

3.3.2. The representative firm

The world's production of final output is represented by a stand-in firm which employs a Cobb-Douglas production technology. The firm hires labor, capital, and energy services from the stand in household and produces the final consumption-investment goods.

The aggregate production function is:

$$Y = \Omega A K^{\alpha} L^{\beta} E^{1-\alpha-\beta} \tag{13}$$

$$\Omega = \frac{1}{(1 + \theta_1 T + \theta_2 T^2)} \tag{14}$$

here, A, is total factor productivity (TFP), and Ω is a climate damage function. We follow Nordhaus (2007), and assume that the damage coefficient is a function of T, global mean temperature. $\theta_1$and θ_2 are parameters of damage function, K is capital stock, L is the population/labor force, and E is industrial CO_2 emission. The sum of the share parameters from the aggregate production function, α and β, are assumed to increase over time, which captures the falling share of energy in GDP.

3.3.3. Government

There is a government in the model that can implement carbon taxes on energy consumption. Government policy is exogenous and consists of a set of fuel specific taxes, τ_i, which depend on the emission intensity of each fuel type i. Finally, $\overline{T}$ is the sum of tax revenues from carbon, which are transferred lump-sum to the household. Then, $P_E E - \overline{T}$ is the household's income from selling energy services to the firm net of taxes.

3.3.4. Energy production

Heat energy and electric energy are produced using fossil fuels and renewables. Aggregate energy services, E, is modeled as a composite good produced from heat energy and electric energy.

Electric energy is produced from fossil fuels, nuclear and hydro power. We assume that nuclear and hydro power are exogenous policy variables. Each period the representative firm solves the following problem:

$$\min_{F_{El,i}} \mathrm{ATC}_{El}\left(F_{El,\mathrm{Coal}}, F_{El,\mathrm{Oil}}, F_{El,\mathrm{Nat.Gas}}\right)$$

Subject to

$$E_{El} \geq \overline{E_{El}}$$

$$P_{El} = \mathrm{ATC}_{El}$$

$$K_{\mathrm{Coal}},\ K_{\mathrm{Oil}},\ K_{\mathrm{Nat.Gas}} \quad \text{given.}$$

where

$$E_{El} = A_{El}\left(a_1 F^{\vartheta}_{El,\mathrm{Coal}} + a_2 F^{\vartheta}_{El,\mathrm{Oil}} + a_3 F^{\vartheta}_{El,3} + a_4 \overline{E}^{\vartheta}_{El,\,\mathrm{Nucl.}} + a_5 \overline{E}^{\vartheta}_{\mathrm{El,\,Hydr.}}\right)^{\frac{1}{\vartheta}}.$$

and

$$a_i = \left(\frac{1}{\omega}\right)\left(g_i - \left(\frac{F_{El,i}}{K_i}\right)^2\right), \quad \text{for } i = 1, 2, 3.$$

In words, given the capital stocks for fossil fuels and the nuclear and hydro power available, the representative firm chooses $\{F_{El,\mathrm{Coal}}, F_{El,\mathrm{Oil}}, F_{El,\mathrm{Nat.Gas}}\}$ to minimize the average total cost of electricity. Here, A_{El} is a productivity term specific to electricity production, $F_{El,i}$ is the fuel input used for fuel type i in electricity production from different sources, $F_{El,i}$ is the fuel input used for fuel type i in electricity production, ATC_{El} is the average total cost of electric energy, $\overline{E_{El}}$ is the threshold value for electric energy, P_{El} is the price of electric energy and ϑ is the CES elasticity parameter (which implies elasticity of substitution of $E_S = 1/(1-\vartheta)$).

The functions a_i, for the fossil fuels, are decreasing in the fuel-to-capital ratio. This reflects diminishing returns, as capital is a fixed factor. The parameters a_4 and a_5 are fixed, while ω and g_i are chosen to match the relative levels of fossil fuels in electricity production.

Heat energy is produced from fossil fuels and alternative energy sources. Each period the representative firm solves the following problem:

$$\min_{F_{H,i}} \mathrm{ATC}_H\left(F_{H,\mathrm{Coal}}, F_{H,\mathrm{Oil}}, F_{H,\mathrm{Nat.Gas}}, F_{H,\mathrm{Alt.}}\right)$$

subject to

$$E_H \geq \overline{E_H} \tag{16}$$

$$P_H = \mathrm{ATC}_H$$

where

$$E_H = A_H\left(b_1 F^{\mu}_{H,\mathrm{Coal}} + b_2 F^{\mu}_{H,\mathrm{Oil}} + b_3 F^{\mu}_{H,\mathrm{Nat.Gas}} + b_4 F^{\mu}_{H,\mathrm{Alt.}}\right)^{\frac{1}{\mu}}$$

There is no capital in the heat energy system component. The capital for heat energy comprises part of the aggregate capital for the economy. The firm chooses $\{F_{H,\mathrm{Coal}}, F_{H,\mathrm{Oil}}, F_{H,\mathrm{Nat.Gas}}, F_{H,\mathrm{Alt.}}\}$ to minimize the average total cost of heat energy. Here, A_H is a productivity term specific to heat energy production, $F_{H,i}$ is the input of fuel type i for heat energy production, b_i is the CES weight for fuel type i, and μ is the CES elasticity parameter.

The fossil fuel price functions are increasing in the ratio of the reserve value at its base year relative to its current value.

$$P_{F_{i,t}} = \tau_{i,t} + P_{F_{i,t=1980}}\left(\frac{R_{i,t} + D_{i,t} - F_{El_{i,t}} - F_{H_{i,t}}}{R_{i,t=1980}}\right)^{\rho} \quad (17)$$

Here, subscripts i and t refer to the fossil fuel type and the year respectively. $P_{F_{i,t}}$ is the fuel price, $\tau_{i,t}$ is the fuel specific carbon tax, $P_{F_{i,t=1980}}$ is the price of fuel at the base year (1980), $R_{i,t}$ is the current reserve level, $R_{i,t=1980}$, is the base year reserve level, and $D_{i,t}$ is the new discovery value. $F_{El_{i,t}}$ and $F_{H_{i,t}}$ is extraction of fuel for electricity and heat energy production respectively. $\rho < 0$ is an elasticity parameter.

Equation (17) implies that the fossil fuel price decreases when the current reserve value falls relative to the base year. Thus the more fuel extracted the higher the price becomes. New discoveries of fossil fuels reduce the price of fossil fuels, holding everything else constant. The paths for new fossil fuel discoveries are prescribed.

The price of alternative heat energy is represented by the function:

$$P_{F_{\text{Alt.},t}} = \mu_{1,t} + F_{H,\text{Alt.},t}^{\mu_{2,t}} \quad (18)$$

$P_{F_{\text{Alt.}}}$ is the price, and $F_{H,\text{Alt.}}$ is the quantity of alternative fuel used in heat energy production. μ_1 and μ_2 are parameters. We assume they are decreasing, so that the price of alternative fuel decreases over time.

3.3.5. Energy demand

Energy demand is derived from the aggregate production function. At period t, the capital and labor inputs are pre-determined. Demand for aggregate energy services can thus be expressed as:

$$E = \left(\frac{(1-\alpha-\beta)AK^{\alpha}L^{\beta}}{P_E}\right)^{\frac{1}{(\alpha+\beta)}} \quad (19)$$

E is the representative firm's demand for aggregate energy services, K is aggregate capital, L is the world's labour force, and P_E is the price of aggregate energy services. α and β are the share parameters from the aggregate production function.

Heat energy and electric energy is combined into aggregate energy services by a CES function:

$$E = \left(\gamma E_H^{\theta} + (1-\gamma)E_{El}^{\theta}\right)^{\frac{1}{\theta}} \quad (20)$$

where E_H is total heat energy produced, and E_{El} is total electricity produced. The elasticity of substitution is determined by the parameter θ, and γ is the CES share parameter.

3.3.6. Investment in capital for electricity production

Investment into new capital for electricity production follows an average cost investment rule and is allocated by a built-in Vensim function called 'Allocate-by-priority' (Ventana Systems, 2010).

Investments in electricity capital I_{El} is a fixed fraction of total investment, and is given by

$$I_{El} = sY\left(\frac{\sum_i K_i}{K + \sum_i K_i}\right) \quad (21)$$

where K_i is the current capital stock used to produce electricity from energy source i, which could be either a fossil fuel, nuclear or hydro power. K is the aggregate capital stock.

For investment in electricity capital, the allocate-by-priority (ABP) function serves as a market clearing mechanism. The ABP function in Vensim is based on the Wood algorithm (Ventana Systems, 2010) for allocating a resource in scarce supply to competing orders or 'requests'. The ABP function takes as inputs the supply of available investment funds to be allocated, and the 'capacity' and the 'priority' of each order, representing the size and competitiveness of the orders respectively.

The ABP function has a 'width' parameter which determines how exclusively the available investment funds will be allocated. The width-parameter can take any positive value. The lower the value of the width the more responsive is the allocation to differences in order priority. For example, if two orders have similar capacitates and priorities, then a high width will produce a very even allocation. On the other hand, as the width parameter decreases, the allocation of investment funds will be shifted towards the order with the higher priority (Ventana Systems, 2010).

Given the fixed quantity of investment funds available inside a period, the market allocation depends on the size of the request and relative priority given to each system component, and the width parameter. In ANEMI_2 the priorities for the system components are set equal to each other, and model only focuses on the request dimension. This simplifies the calibration and makes the investment function more transparent.

The demand for new investment funds for each energy source used in electricity production is based on an average cost investment rule where the allocation is determined by the ABP function. Given a fixed priority across energy sources, the 'request' function (Req_i) takes the following form:

$$\text{Req}_i = \phi_i\delta_i K_i + \left(\frac{K_i}{\sum_i K_i}\right)\left(\frac{\text{ATC}_{El}}{\text{ATC}_i}\right) \quad (22)$$

The request for new investment funds is a function of 'replacement capital' and the current capital share of the system component scaled by its relative average total cost. Each period a share δ of existing capital depreciates, and we assume that all system components will ask for that capital to be replaced. The parameter φ is a weighting factor that will reduce the request for replacement capital if the average total cost exceeds some threshold value. The second term is the relative size of the current capital stock for energy source i multiplied by its relative average cost. This implies that system components with a lower average cost will have higher requests. ATC_{El} is the average total cost of electricity, and ATC_i is the average total cost of energy source i.

Note that, as the path for nuclear and hydro power is given exogenously, the capital stock used in production of nuclear and hydro power is also prescribed. The amount needed for new capital for nuclear and hydro power is first subtracted from the total amount available for investment into electricity capital; what is left over is allocated to the fossil fuel capital stocks using the ABP function.

3.4. Climate system component

The climate system component of the ANEMI_2 model simulates the atmospheric and oceanic temperature changes caused by the increase in anthropogenic CO_2 concentration. There are two versions of the climate system component in the ANEMI_2 model. The first is the modified form of ANEMI_1 climate system component (for details see Davies, 2007; Davies and Simonovic, 2008;

Akhtar et al., 2011) that is based on the upwelling-diffusion energy-balance model (UD/EBM) that builds on the Box Advection-Diffusion (BAD) model of Harvey and Schneider (1985). The second version is adopted from the DICE model of Nordhaus (1994, 2007), and is much simpler than the BAD model.

The simplified setup of the ANEMI_2 climate system component (Fig. 5) is based on the DICE model (Nordhaus, 1994, 2007, 2008), and is used for computing atmospheric and oceanic temperature. Nordhaus used a second-order, linear system with three negative feedback loops. The first loop describes the warming of the ocean while the remaining two describe the transmission of heat from the atmosphere and ocean surface respectively.

Since the ocean has a large heat capacity, deep Ocean warming is a slow process. In the ANEMI_2 model, radiative forcing from CO_2 is expressed as a logarithmic function of the atmospheric CO_2 concentration. Forcing from other gases is exogenous, based on the IPCC assumptions used by the DICE model (Nordhaus, 1994). The equilibrium temperature response to a change in radiative forcing is determined by the radiative forcing coefficient and the climate feedback parameter.

The climate system component includes two major feedbacks producing radiative forcing that increases temperature. In the climate system component, the atmospheric CO_2 is translated in the radiative forcing according to the forcing equation. The sources of radiative forcing are also computed from other gases, including methane, nitrous oxide, chlorofluorocarbons, and other Montreal protocol gases. Total forcing is then obtained as the input into the climate system component according to:

$$F_{\text{total}} = F_{CO_2} + F_{\text{other}} \tag{23}$$

$$F_{CO_2} = S \cdot \frac{\ln\left(\frac{C_A}{C_{A0}}\right)}{\ln(2)} \tag{24}$$

$$F_{\text{other}} = F_{\text{cfc}} + F_{CH_4} + F_{N_2O} + F_{\text{MP}} \tag{25}$$

where F_{total} is for total forcing in W m-2; F_{CO_2}, F_{cfc}, and F_{N_2O} stand for radiative forcing from carbon-dioxide, chlorofluorocarbon and nitrous oxide respectively. F_{MP} represents Montreal Protocol and other gases; while C_A and C_{A0} denote the current and the initial atmospheric carbon dioxide concentrations respectively.

The simpler version of the climate system component model uses temperature gradient and the heat absorption capacity of the deep ocean to represent the transmission of heat from the atmosphere and the upper ocean layer to the deep ocean. For the sake of simplicity, the model here consists of 2 layers, one includes the atmosphere and the upper ocean and the other includes the deep ocean. One of the main contributors of temperature change in both of these layers is radiative forcing produced from CO_2 and other GHGs including CH_4 (methane), NO_2 (nitrous oxide), and CFC (chlorofluorocarbon).

The transformation of GHGs (specifically CO_2) to equivalent temperature is calculated by,

$$T_{\text{equil}} = \frac{k \ln\left(\frac{C_a}{C_{a,0}}\right)}{\lambda \ln(2)} \tag{26}$$

where T_{equil} refers to equilibrium temperature, C_a is atmospheric CO_2 concentration, $C_{a,0}$ is preindustrial atmospheric CO_2 concentration, k is radiative forcing coefficient (4.1 W m^{-2}), and λ is climate feedback parameter (1.41 W/m^2 °C).

Unlike the BAD-based comprehensive model, the simplified version consists of only two layers. The temperature of the atmosphere and upper ocean layer is given by

$$T_{\text{AUO}} = \int CT_{\text{AUO}} \cdot dt \tag{27}$$

where temperature of the atmosphere and upper ocean is expressed as T_{AUO}, and CT_{AUO}.

Deep ocean layer temperature is calculated by Nordhaus (1994, 2007) as

$$T_{\text{DO}} = \int CT_{\text{DO}} \cdot dt \tag{28}$$

where T_{DO} is the temperature of the deep ocean and CT_{DO} is the change of temperature in the deep ocean layer. The first layer (the atmosphere and upper Ocean) temperature change is computed with the help of radiative forcing, heat transfer and the heat capacity of the atmosphere and upper ocean:

$$CT_{\text{AUO}} = \frac{F - f_H - HT}{HC_{\text{AUO}}} \tag{29}$$

where CT_{AUO} is the temperature change at the atmosphere and upper ocean, F is radiative forcing, f_H is the feedback from heating,

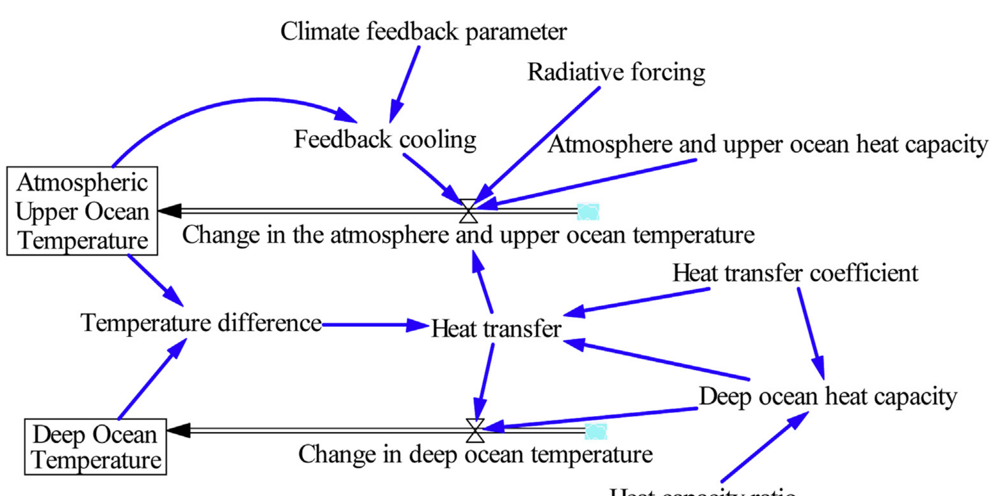

Fig. 5. Simplified climate system component of ANEMI_2 model (after Nordhaus, 1994, 2007).

HT is for heat transfer from the atmosphere and upper ocean to the deep ocean, and HC_{AUO} denotes the heat capacity of the atmosphere and upper ocean layer.

The temperature change of the deep ocean layer depends upon the heat capacity of the deep ocean and the heat transfer rate between the two layers.

$$CT_{DO} = \frac{HT}{HC_{DO}} \tag{30}$$

where CT_{DO} is the temperature change in the deep ocean layer, *HT* is the heat transfer from the atmosphere and upper ocean layer to the deep ocean layer, and HC_{DO} is the heat capacity of the deep ocean layer.

Heat capacity of the deep ocean is calculated by the following equation

$$HC_{DO} = R_{HC} \cdot C_{HT} \tag{31}$$

where HC_{DO} is the heat capacity of the deep ocean layer, R_{HC} is the heat capacity ratio and C_{HT} stands for heat transfer coefficient.

The heat transfer between the two layers mainly depends on the temperature gradient, the heat transfer coefficient and the deep ocean's heat absorption capacity. Heat transfer between the layers is thus computed by

$$HT = (T_{AUO} - T_{DO})\left(\frac{HC_{DO}}{C_{HT}}\right) \tag{32}$$

where *HT* is the heat transfer from the atmosphere and upper ocean to the deep ocean, T_{AUO} and T_{DO} denote the temperature of atmosphere and upper ocean layer and the deep ocean layer, respectively. C_{HT} represents the heat transfer coefficient and HC_{DO} stands for the deep ocean heat capacity.

3.5. Other modifications incorporated in the ANEMI_2 model

The final version of ANEMI_2 model incorporates a few modifications that did not require addition of new system components, rather the expansion of existing system components. These modifications include CO_2 solubility in seawater, addition of sea-level rise, and addition of green water (the portion of the rainfall that is intercepted by vegetation, taken up by plants to create biomass and then evapotranspirated back into the atmosphere). They are presented in this section.

A. Carbon dioxide is easily dissolved in seawater, and its solubility is temperature dependent. Colder water can dissolve more CO_2, while higher water temperature reduces the solubility according to Henry's Law. Henry's Law states that CO_2 is in equilibrium between air and water at 25 °C when approximately 1/50 of the gas is in the air and the remaining gas is dissolved in the water. If 50 units of gas are added to the air 49 units will thus be dissolved into the water.

Therefore the temperature dependent solubility of CO_2 in water is incorporated in the carbon system component of the ANEMI_2 model, which influences the ocean's carbon absorption rate. Akhtar (2011, Fig. 3.7, page 68) used relationship between the CO_2 solubility of ocean water (from 0.5 to 100 MPa) and the temperature (from 0 to 100 °C).

$$CO_2 \text{ from atmosphere to ocean} = f\left\{\text{temperature}, \left(\frac{\text{equilibriun carbon in the mixed layer} - \text{carbon in mixed layer}}{\text{Mixing time}}\right)\right\} \tag{33}$$

B. In order to deal with global water resources, the ANEMI_2 model incorporates another important water-related system component: sea-level rise. This system component is introduced into the model in order to understand more clearly the feedback relationships between climate, water, and land-use system components.

There are processes in several nonlinearly coupled components of the Earth system that contribute to sea-level change. The climate change on decadal and longer time scales alters the volume of water in the global ocean by: (i) thermal expansion, and (ii) the exchange of water between oceans and other reservoirs (glaciers and ice caps, ice sheets and other land water reservoirs) (IPCC, 2007c). Vertical land movements such as glacial isostatic adjustment, tectonics, subsidence and sedimentation may influence local sea-levels, but they do not alter ocean water volume.

The global sea-level rise is estimated to be about 120 m during the several millennia of the last ice age (approximately 21,000 years), and stabilized between 3000 and 2000 years ago (IPCC, 2007c). Indicators such as marine deposits and lower boundary of mangrove growth show that the global sea-level did not subsequently change in any significant way until the late 19th century. Estimates for the 20th century showed that the global average sea-level rise is occurring at a rate of about 1.7 mm/yr. It is believed that over the period from 1961 to 2003, thermal expansion contributed on average to about half of the observed sea-level rise, while melting of the land ice accounted for less than half. Granted, there is some uncertainty in these estimates.

Understanding global sea-level change is a rather difficult scientific problem. It includes complex mechanisms and a large number of feedback relationships. Significant uncertainties persist, even in the projection of thermal expansion. For example, the 4th Assessment Report of Intergovernmental Panel on Climate Change (IPCC) did not include rapid ice flow changes in the projected sea-level rise. IPCC stats that modeling of this phenomenon is not completed yet and consequently the upper limit of the expected rise is not included in the report. This leads to the consideration of semi-empirical approaches for the projection of sea-level rise. These approaches are based on using observable variable that climate models can predict with confidence, like global mean temperature, and establish, with the help of observations a link between the global mean temperature and sea-level change. Therefore, semi-empirical models provide a pragmatic alternative for estimation of the sea-level response to changing climatic conditions. The gravity measurements conducted from space have revealed that the mass loss from Greenland and Antarctic ice sheets is accelerating with time and more closely approximates a quadratic trend than the linear one. Many recent references (Church and White, 2006;

Overpeck and Weiss, 2009; Vermeer and Rahmstorf, 2009; Jevrejeva et al., 2010) are projecting more than 1 m seal-level rise by the end of this century.

In the ANEMI_2 model, the global average near surface air temperature is considered as the driver for sea-level change. Following Rahmstorf (2007), the sea-level rises as the ocean takes up heat and ice starts to melt, and continues to rise asymptotically until a new equilibrium sea-level is reached. Paleoclimatic data suggest that changes in the final equilibrium level may be very large. The sea-level at the last glacial maximum (about 20,000 years ago) was 120 m lower than the current level, where global mean temperature was 4–7 °C lower (Von Deimling et al., 2006; Waelbroeck et al., 2002). Three million years ago, during the Pliocene epoch, the average climate was about 2–3 °C warmer and sea-level was 25–35 m higher than today's value (Rahmstorf, 2007; Dowsett et al., 1994). These data suggest changes in sea-level on the order of 10–30 m per °C (Rahmstorf, 2007).

For the most part, the initial rate of rise is to be proportional to the temperature increase,

$$\frac{dH}{dt} = a(T - T_0) \tag{34}$$

where H is the global mean sea-level, t is time, a is the proportionality constant, T is the global mean temperature, and T_0 is the previous equilibrium temperature value. The equilibration time scale is expected to be in the order of millennia. As long as the linear approximation holds, the sea-level rise from the previous equilibrium state can be computed by the following equation:

$$H(t) = a\int_{t_0}^{t}\left(T\left(t'\right) - T_0\right)dt \tag{35}$$

where t' is the time variable.

Rahmstorf (2007) established a highly significant correlation of global temperature and sea-level rise ($r = 0.88$, $P = 1.6 \times 10^{-8}$) with a slope of $a = 3.4$ mm/year per °C. The baseline temperature T_0, at which sea-level rise is zero, is 0.5 °C below the mean temperature for the period 1951–1980.

C. Green water consumption in the global agriculture system component is incorporated to reflect the water quality effects for rainfed cropland runoff on water-stress. Green water is the portion of the rainfall that is intercepted by vegetation and by the soil, and is taken up by plants to create biomass and then evapotranspirates into the atmosphere. The ANEMI_2 model computes the volume of runoff from rainfed cropland and pasture as an area-weighted fraction of the total runoff from the land surface. The fresh water requirements to dilute agrochemicals (which are used on the rainfed cropland) is computed by multiplying the "rainfed cropland runoff" with the "green water" dilution multiplier.

In some regions, food production almost entirely depends on the green water (for example, >95% in sub-Saharan Africa). Green water is important for irrigated land, as addition to blue water (the part of the rainfall that moves through the hydrological cycle and ends up in rivers, lakes and groundwater – the water that we primarily manage and use.) that supplements the available precipitation required for ensuring optimal crop growth. Hence, the global agricultural water consumption is much higher than suggested by figures that refer to blue water use only. The importance of green water is demonstrated by Rost et al. (2008). Their work strengthens the need for including green water flows in the assessments of global water resources and water scarcity. Green water can be broadly classified into green crop water and green pasture water. Green crop water is basically the overland flow/runoff that comes from agricultural areas which are not under irrigation (rainfed agricultural area). Green pasture water is the flow from pasture land.

The rainfed cropland (A_{RCA}) can be computed by deducting the irrigated area (A_{tirr}) from the total agricultural land (A_{arable}) as,

$$A_{RCA} = A_{arable} - A_{tirr} \tag{36}$$

while for computing the rainfed cropland runoff, area-weighted method is used considering the equal distribution of runoff over the total biome area. Therefore, the rainfed cropland runoff (Q_{RCR}) is

$$Q_{RCR} = Q_S \cdot \left(\frac{A_{RCA}}{A_{tbio}}\right) \tag{37}$$

where Q_S is the total renewable flow, and A_{tbio} is the total biome area.

The green crop water dilution requirement is the amount of fresh water required to dilute polluted crop water. On the basis of the studies done by Chapagain et al. (2006) and Dabrowski et al. (2009), the dilution requirement of the green crop water is assumed to be 1:1. So, the green crop water dilution requirement (Q_{gcwdr}) can be formulated as follows,

$$Q_{gcwdr} = Q_{RCR} \cdot F_{gcwd} \tag{38}$$

Since the green crop water dilution requirement factor (F_{gcwd}) is considered as 1, the Equation (38) can be rewritten as

$$Q_{gcwdr} = Q_{RCR} \tag{39}$$

However, the computation of green water from pasture land is not as straightforward as the computation of green water from rainfed cropland. This is due to the complexity in determining total pasture land. In the ANEMI_2 model pasture land is calculated based on the requirements for increased animal production as a portion of the food supply for the growing population. Pasture land productivity is therefore a function of the increase in human food production (P_{ipfood}) and pasture land area (A_{Pa}). The calculation of animal product takes the following form

$$A_{Pa} = \frac{\left(f\left(P_{ipfood}\right)\right) \cdot dt}{Y_{A_{Pa}}} \tag{40}$$

where $Y_{A_{Pa}}$ is the average yield from pasture land.

Runoff from the pasture land is computed in a similar fashion as the runoff for the cropland. So the simplified form of the pasture land runoff (Q_{PaR}) calculation is

$$Q_{PaR} = Q_S \cdot \left(\frac{A_{Pa}}{A_{tbio}}\right) \tag{41}$$

where Q_S is the total renewable flow, and A_{tbio} is the total biome area.

The green pasture water is less polluted than the green cropland water. In this study it is assumed to be 1/10 of the cropland water. The green pasture water dilution requirement (Q_{gpadr}) can be then written as

$$Q_{gpadr} = Q_{PaR} \cdot F_{gpad} \tag{42}$$

As the green crop water dilution requirement is assumed only 10% of the (F_{gcwd}) polluted water, so the dilution requirement

(F_{gpad}) will be 0.1 and the simplified form of the Equation (42) will be

$$Q_{gcwdr} = 0.1Q_{RCR.} \tag{43}$$

The dilution requirement for the domestic and industrial waste water is computed based on the typical value of three main pollutants, BOD_5, total nitrogen, and total phosphorous, and their corresponding acceptable values. For domestic waste water

$$\mathrm{Dil}_D = \mathrm{Max}\left(\frac{DTy_{\mathrm{BOD}_5}}{Ac_{\mathrm{BOD}_5}}, \frac{DTy_{\mathrm{tot\ N}}}{Ac_{\mathrm{tot\ N}}}, \frac{DTy_{\mathrm{tot\ P}}}{Ac_{\mathrm{tot\ P}}}\right) \tag{44}$$

$$\mathrm{Dil}_I = \mathrm{Max}\left(\frac{ITy_{\mathrm{BOD}_5}}{Ac_{\mathrm{BOD}_5}}, \frac{ITy_{\mathrm{tot\ N}}}{Ac_{\mathrm{tot\ N}}}, \frac{ITy_{\mathrm{tot\ P}}}{Ac_{\mathrm{tot\ P}}}\right) \tag{45}$$

where Dil_D and Dil_I are dilution requirements for domestic and industrial waste water respectively. AC_{BOD_5}, $Ac_{\mathrm{tot\ N}}$, and $Ac_{\mathrm{tot\ P}}$ are acceptable values of discharged treated water for five-day biochemical oxygen demand, total nitrogen, and total phosphorous respectively. DTy and ITy are typical values of the domestic and industrial waste water respectively (pollutant concentration).

4. Sensitivity analyses

The scientific knowledge of the Earth-system behavior is available today for the development of an appropriate mathematical model with rigorous system description (mathematical formulation) and reasonable set of parameter values. However, there is always room for improvement of model behavior by increasing the accuracy of model parameters. Influence of model parameters could vary from minor to significant. The sensitivity analyses can be helpful in the development of more robust models. With the help of sensitivity analyses the key modeling assumptions can be tested by altering the assumed values in successive simulations and then examining the resulting output. When sensitive components come from well-understood elements of the Earth-system, their sensitivity is either expected and its limits are generally well-known, or it stems from unforeseen feedback linkages and comes as something of a surprise (Davies, 2007). However, it can be explained relatively easily in retrospect.

The ANEMI_2 model is based on previous modeling work. Hence, many of its components have the same parameter values as other models. In cases where the parameters are derived from well-established, quantifiable, and measurable characteristics, we have checked the values used in the model against the real-world data. However, in cases where the parameters did not have the strong physical basis, we checked their impacts on model behavior through the sensitivity analyses. Since the main objective of this research is to improve our understanding of global system by investigating 'what if' scenarios rather than replicating the real-world behavior, the two main sensitivity approaches can be implemented: 1) simulation comparisons between extreme and a base runs, and 2) Monte Carlo simulation.

The ANEMI_2 model is based on a very complex structure due to a higher number of nonlinear system equations and the use of integrated simulation - optimization scheme. Therefore, the simplest method of sensitivity analysis has been implemented by repeatedly varying one parameter at a time while holding the other parameters fixed. This is a powerful test of sensitivity that takes into account the parameter's variability and the associated influence of a selected parameter on the model output. The results of sensitivity analyses are presented in Table 1.

The imposed population system component parameter-variations in the sensitivity analyses result in the largest changes in simulated surface temperature, which affects the food availability (food per capita) in the food production system component. However, the variability in the technological development delay and average life of the land show very limited (in some cases negligent) effect on the atmospheric carbon dioxide concentration, global temperature, population and the other variables in the food system component. The sensitivity analyses of the desired food ratio (within the food system component) resulted in the most significant changes in the population system component, which then caused a change in global CO_2 emission values.

5. Potential application: three scenario experiments

The assessment reports from the Intergovernmental Panel on Climate Change (IPCC, 2007b; Trenberth et al., 2007; Schneider et al., 2001) have identified the key potential impacts of climate change. Furthermore, these reports point to human-induced increases in the atmospheric concentration of greenhouse gasses (GHGs) as a likely cause of climate change. There is a relatively strong consensus in the scientific community that GHGs emissions need to be cut in order to reduce the impacts of climate change.

To illustrate the potential applications of ANEMI_2, we examine three policy scenarios to reduce GHG emissions (Popovich et al., 2010). The first scenario focuses on the impact of a carbon tax.

Table 1
Comparison of changes in major variables (in percent) as a result of sensitivity analyses.

Parameter	Population (change compared to base run, %)	Food per capita (change compared to base run, %)	Water stress (change compared to base run, %)	Total CO2 emission (change compared to base run, %)	Global temperature (change compared to base run, %)
Year 2025					
Desired food ratio (−25% to +25%)	−4.5 to 0.1	−17 to 3	−1 to 0	−1.7 to 0.16	−0.01 to 0
Average life of the land (−17%–33%)	−0.03 to 0.03	−0.09 to 0.11	−0.01 to 0.01	−0.01 to 0.02	0
Technological development delay (−40%–40%)	1.4 to −1.4	1.1 to −1.5	0.5 to −0.4	0.7 to −0.6	0
Reproductive lifetime (−17%–17%)	15 to −12	−11 to 8	6.4 to −4.7	8.5 to −7.4	−0.03 to +0.03
Year 2050					
Desired food ratio (−25% to +25%)	−9 to 3	−23 to 18	−3 to 1	−6 to 2	−0.06 to 0.01
Average life of the land (−17%–33%)	−0.04 to 0.05	−0.10 to 0.12	−0.01 to 0.02	−0.02 to 0.03	0
Technological development delay (−40%–40%)	0.9 to −0.8	−0.14 to −0.2	0.4 to −0.5	0.3 to −0.3	0.01 to −0.01
Reproductive lifetime (−17%–17%)	18 to −16	−7 to 8	8 to −8	11 to −14	0.2 to −0.02
Year 2075					
Desired food ratio (−25% to +25%)	−12 to 6	−24 to 23	−4.2 to 1.6	−5.1 to 3.2	−0.16 to 0.05
Average life of the land (−17%–33%)	−0.05 to 0.06	−0.1 to 0.1	−0.01 to 0.02	−0.01 to 0.0	0
Technological development delay (−40%–40%)	0.6 to −0.5	−0.5 to 0.6	0.3 to −0.3	−0.6 to 0.4	0.02 to −0.02
Reproductive lifetime (−17%–17%)	24 to −19	−2.6 to 3.4	8.0 to −9.0	3.6 to −4.2	0.4 to −0.5

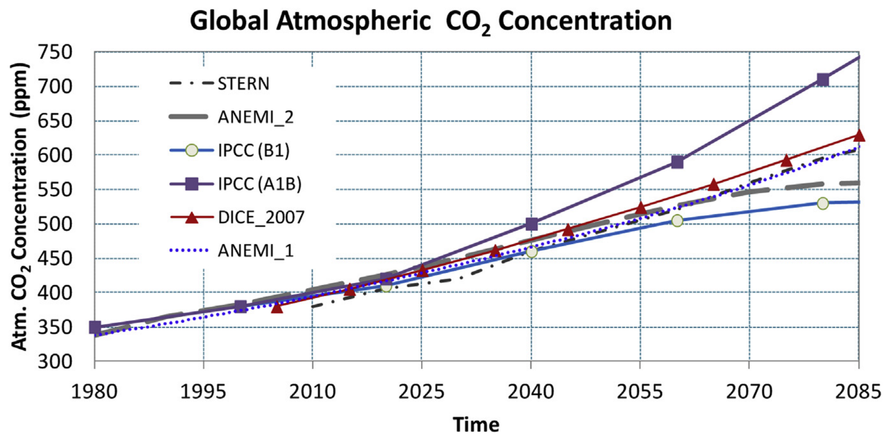

Fig. 6. Global atmospheric CO_2 concentration.

The second scenario looks into global increase of water use. The third scenario describes the increase in global food production. These scenarios are selected to illustrate the model use and performance and are not based on the real internationally available policy scenarios.

All three scenarios are compared with the baseline scenario. The baseline/baseline scenario is any datum against which change is measured. In the ANEMI_2 simulations, the baseline scenario integrates the historical observations with a set of parameter values. In this study all the model system components are calibrated with the observations and then the model simulations produce the dynamic behavior of all state variables. The baseline scenario represents business as usual, and is based on commonly used projections from the scientific community (Akhtar, 2011; Akhtar et al., 2011). A sample comparison of the global atmospheric CO_2 concentration is presented in Fig. 6 and for the rest of the parameter comparison readers are referred to the listed publications.

Apart from the above mentioned scenarios a high energy intensive scenario has been introduced by increasing the energy reserve to a significant amount (25 percent) and pushing the population growth rate little bit higher (6 percent more compared to base condition by the year 2085), which will be discussed in Section 5.4.

5.1. Carbon tax scenario

This scenario assumes that a carbon tax is implemented in 2012 and slowly ramped up to $100 per tonne of CO_2 over 30 years. Fig. 7 show how the implementation of the carbon tax affects the electric and heat energy production. The dashed lines in these figures show the ANEMI_2 simulation results without the carbon tax, and the full lines show the results with the carbon tax in place. The carbon tax has a significant impact on heat energy production which relies on fossil fuel as the energy input. However, the carbon tax has less of an effect on electricity production, which relies more on nuclear and hydro power.

The carbon-tax policy lowers the amount of carbon emissions in the production of each unit of energy. This occurs since the carbon tax increases the relative price of carbon intensive fossil fuels, which leads energy producers to substitute towards less carbon intensive fuels. In addition, the increase in the price of energy leads to a dramatic drop in energy consumption.

As can be seen from Table 2, this changes the dynamics of the global energy-economy system component. In the baseline, world fossil fuel (natural gas and oil) reserves decline to very low levels by 2080. In turn, fossil fuel prices rise as reserves decline, which leads to both less intensive use of energy in the economy and more use of alternative energy sources. The initial reduction in fossil fuel based energy consumption after the implementation of the carbon-tax implies a slower decrease in the stock of fossil fuel reserves. This slower decrease in reserves in turn means that fossil fuel prices (net of carbon taxes) rise more slowly, as the cost of fossil fuel production (extraction) is decreasing in reserves. This results in a more stable supply of fossil fuel based energy throughout the 21st century. Such behavior is driven by the availability of the fossil fuel reserve.

This shift in the timing of consumption of fossil fuel leads to a shift in the time path of emissions (see Table 2). Thus, the carbon tax policy postpones emissions from fossil fuels, but does not eliminate them. This highlights one of the key advantages of the

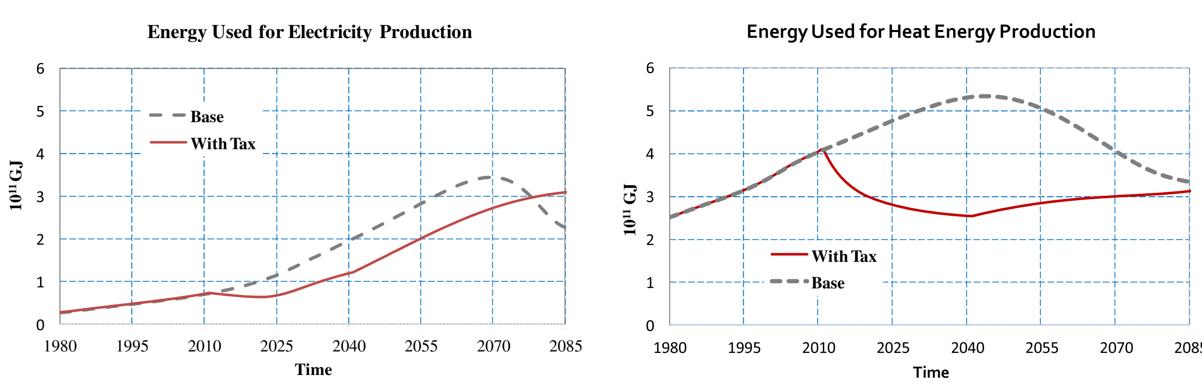

Fig. 7. Energy used to produce electricity (left) and heat (right) energy.

Table 2
ANEMI_2 Model Simulation Result.

Variables	Scenario	1980	1990	2000	2010	2025	2050	2075	2085
Food Production (*Trillion kilocalorie/yr*)	Baseline	2455.47	3026.26	3872.58	5460.76	8652.45	12,198.94	14,749.08	15,403.54
	Carbon tax	2455.47	3026.26	3872.58	5460.76	9175.13	13,568.44	15,995.85	15,925.72
	Water use increase	2455.47	3026.26	3872.58	5460.76	8425.97	11,828.96	14,023.99	14,532.79
	Food production increase	2455.47	3026.26	3872.58	5460.76	8705.41	12,465.98	14,925.06	15,531.22
Available surface water (km^3)	Baseline	15,203.7	15,275.86	15,316.81	15,343.65	15,409.55	15,549.13	15,692.21	15,756.03
	Carbon tax	15,203.7	15,275.86	15,316.81	15,343.65	15,410.74	15,525.75	15,614.65	15,652.26
	Water use increase	15,203.7	15,275.86	15,316.81	15,343.65	15,347.60	15,449.72	15,581.67	15,640.99
	Food production increase	15,203.7	15,275.86	15,316.81	15,343.65	15,400.01	15,516.74	15,637.64	15,692.48
Water stress (*unit less*)	Baseline	0.33	0.360	0.403	0.460	0.512	0.567	0.611	0.603
	Carbon tax	0.33	0.360	0.403	0.460	0.500	0.531	0.590	0.600
	Water use increase	0.33	0.360	0.403	0.460	0.552	0.605	0.645	0.635
	Food production increase	0.33	0.360	0.403	0.461	0.516	0.580	0.633	0.629
Population (*Billion*)	Baseline	4.437	5.130	5.909	6.766	7.982	9.318	9.972	10.259
	Carbon tax	4.437	5.130	5.909	6.766	8.173	10.294	11.196	11.331
	Water use increase	4.437	5.130	5.909	6.766	7.842	8.900	9.400	9.609
	Food production increase	4.437	5.130	5.909	6.766	7.971	9.275	9.847	10.091
CO_2 emission from fossil fuel (*Gt*)	Baseline	19.008	22.099	25.485	28.871	32.849	38.290	25.336	15.364
	Carbon tax	19.008	22.099	25.485	28.871	14.963	14.738	15.930	13.819
	Water use increase	19.008	22.099	25.485	28.871	32.542	36.657	24.689	14.532
	Food production increase	19.008	22.099	25.485	28.871	32.828	38.144	25.172	15.149
GDP (*trillion $*)	Baseline	18.260	27.895	37.641	55.789	94.468	181.967	274.138	308.601
	Carbon tax	18.260	27.895	37.641	55.789	95.377	191.801	308.503	357.8847
	Water use increase	18.260	27.895	37.641	55.789	93.731	175.447	260.253	291.043
	Food production increase	18.260	27.895	37.641	55.789	94.417	181.3728	271.681	304.796
Atmospheric CO_2 concentration (*ppm*)	Baseline	338.72	362.56	382.88	404.27	437.61	502.06	553.24	559.74
	Carbon tax	338.72	362.56	382.88	404.27	422.88	438.82	462.86	470.87
	Water use increase	338.72	362.56	382.88	404.27	437.29	498.84	546.71	553.07
	Food production increase	338.72	362.56	382.88	404.27	437.84	504.43	558.56	566.31
Atmospheric temperature ($^\circ C$)	Baseline	14	14.22	14.46	14.69	15.04	15.62	16.22	16.43
	Carbon tax	14	14.22	14.46	14.69	15.02	15.48	15.92	16.08
	Water use increase	14	14.22	14.46	14.69	15.04	15.61	16.21	16.41
	Food production increase	14	14.22	14.46	14.69	15.04	15.62	16.23	16.45
Energy consumption (*Billion GJ*)	Baseline	269.94	318.15	370.05	420.41	481.68	593.51	416.84	217.66
	Carbon tax	269.94	318.15	370.05	420.41	228.77	254.87	294.52	258.67
	Water use increase	269.94	318.15	370.05	420.41	447.20	569.25	412.35	216.35
	Food production increase	269.94	318.15	370.05	420.41	481.37	591.32	414.93	216.16
Sea-level rise (*cm*)	Baseline	−1.70	0	3.735	9.043	19.482	45.560	81.55	95.605
	Carbon tax	−1.70	0	3.735	9.043	18.76	39.34	67.50	79.56
	Water use increase	−1.70	0	3.735	9.043	19.47	45.57	80.66	94.54
	Food production increase	−1.70	0	3.735	9.043	19.492	46.076	82.249	96.572

ANEMI_2 model, by considering the price of resource fuels as endogenous it illustrates how policies that lower emissions today can increase future emissions by shifting the price of fossil fuels.

This scenario also highlights a (well recognized) source of uncertainty about the impact of carbon taxes: the cost of carbon capture and storage. The scenario assumes that carbon capture and storage is available at a cost per tonne of $ 40. This threshold is triggered in the carbon tax scenario after 2030, when the carbon tax becomes high enough to make carbon capture and storage technology competitive. This has a significant impact on the utilization of coal based energy and emissions. If less effective (i.e. more costly) carbon capture and storage is assumed, atmospheric emissions are higher and the economic impact on GDP of carbon taxes are larger.

The nearly 50% decline in fossil fuel based emissions over 2010–2070 in the carbon tax scenario compared to the baseline significantly impacts the climate. Since the main source of anthropogenic emissions is the burning of fossil fuel and forest cutting/burning, lower emissions result in lower atmospheric CO_2 concentration increment rate. As a result, by 2085 the global atmospheric concentration in the carbon tax simulation is close to 470 ppm (Table 2). Lower atmospheric CO_2 concentration leads to lower radiative forcing than in the baseline. This results in a drop of around 0.4 °C in atmospheric temperature by 2085, compared to the baseline (Table 2). Additional results, shown in Table 2, point to slowing down of sea-level rise when compared to the baseline scenario.

The smaller rise in temperature and decreased pollution in the carbon tax scenario result in higher human life expectancy than in the baseline. Global population thus increases by almost 10% over the following 50 years relative to the baseline (see Table 2). This leads to higher demand for food production, which in turn results in higher water demand for irrigation. As more irrigation produces higher water pollution, water-stress rises faster than in the baseline (even though the magnitude is still lower) as more fresh water is required for dilution (see Table 2). This eventually acts as a negative feedback force in the food production and population system components.

The impact of the carbon tax on GDP per capita is initially negative (from 2012 to 2017), because of the distortion created by higher energy prices due to the carbon tax policy (Table 2). Over time, the benefits from the lower climate damage (which lower GDP per capita) and cheaper fossil fuel in later periods (due to slower depletion of fossil fuel reserves) offset the tax distortion effect. World GDP is roughly 10% higher in the carbon tax than the baseline by 2085, with most of this difference being due to a larger population.

5.2. Water use increase scenario

With increasing population and rising global temperature, total demand for water rises irrespective of the individual system component water use (domestic, industrial and agricultural). Global increase in water demand results in the demand for additional infrastructure (dams, reservoirs, and diversions). Many watersheds now have their water resources fully allocated, and greater irrigation efficiency will be required if the total irrigated area is to expand in the future while maintaining acceptable stream flows for other uses. Decreasing water availability, declining water quality, and growing water demand are posing significant challenges to human population and the health of ecosystems as well. The IPCC (Kundzewicz et al., 2007) states that global warming will lead to “changes in all components of the freshwater system,” and concludes that “water and its availability and quality will be the main pressures on, and issues for, societies and the environment under climate change” (Bates et al., 2008). In areas where crops are now receiving insufficient water for optimum growth, improved irrigation efficiencies may actually dictate an increase in irrigation water used per unit of land. For example, in Alberta and British Columbia (Canada), studies of irrigation system practices found that for some crops, producers were under-irrigating and could improve production by increasing the amount of water applied. Climate change projections for Canada indicate a 37% increase in irrigation water demand in the Okanagan Valley, B.C. (Neilsen et al., 2001). At the same time, continued improvement in irrigation and conveyance efficiency will free up some water for other uses.

Therefore, the second policy scenario included in this research focuses on the increase in water use. The ANEMI_2 model thus tested an assumed amount of 15% increase across all water uses for the purpose of illustrating model utility.

The main impact of a 15% increase in water consumption from the base conditions is a 1% decrease in available surface water (Table 2). This value may seem negligible on a global scale but in terms of agriculture and domestic use, it translates into a 0–50% decrease. The increase in global water stress, which does not account for spatial variability of water supply and use, is around 6%.

The increase in water withdrawals corresponds to a decrease of water quality and eventually produces even higher water-stress (due to increase in dilution requirements). The agricultural system component faces higher water scarcity and reduction in food productivity of more than 5% (Table 2).

The increase in water-stress poses a threat to human survival, especially in terms of life expectancy, since it entails a reduction of per capita food production. Therefore, these two combined feedbacks—increasing water stress and decreasing food production—result in a 7.5% reduction of the overall population by 2085. The global GDP also decreases, but at a very nominal level (2.5%) due to the decrease in the global population (Table 2).

With the reduction of the global population, the CO_2 production from fossil fuel emissions decreases, and so does the atmospheric CO_2 concentration (Table 2). Atmospheric CO_2 concentration is one of the major driving sources of radiative forcing. It is largely responsible for the global temperature rise. Since the atmospheric CO_2 concentration exhibits negligible change, the model does not show any significant change in the atmospheric temperature or in the sea-level rise (Table 2).

5.3. *Food production increase scenario*

In a recent news release, the Food and Agriculture Organization of the United Nations stated that “…Producing 70 percent more food for an additional 2.3 billion people by 2050 while at the same time combating poverty and hunger, using scarce natural resources more efficiently and adapting to climate change are the main challenges world agriculture will face in the coming decades…” (FAO, 2009).

This scenario is closely related to the higher water use scenario. Whereas the water use scenario experiments with the impact of increasing irrigation to cope with rising food demand, the food production scenario tests the impact of redistributing the land-use, by converting more land from forest into agriculture land. This illustrates the richness of the ANEMI_2 model, as it shows how increased pressure on the world’s agricultural system component may impact the sink capacity of the land, and produces output in various system components—namely, population, hydrologic cycle, water quality, energy-economy, climate, carbon, and food production.

Although it is desirable to incorporate as many combinations of crops, livestock and production technologies as possible, we have to keep in mind the model complexity. Every addition increases the difficulty in interpretation of simulation results. The possible number of combinations of cropping patterns and livestock and the degree of sustainability of land units is very large and arbitrary choice has to be made. The feedback based ANEMI_2 model has a high level of complexity already by representing nine system components in an integrated fashion.

The simulation results (shown in Table 2) demonstrate that a 15% increase in agricultural land conversion results in a 1% increase in food production at the beginning of the policy implementation period. However, the extra production slowly starts to decline because of the water shortage.

It is important to note that more than 80% of the projected land expansion is expected to take place in sub-Saharan Africa and Latin America. (By contrast, there is little room for expansion of the agricultural area in South Asia and Near East/North Africa, where almost all the suitable land is already in use.) One fourth of the expanded agricultural land is assumed to be under irrigation. This increases agricultural water consumption and thereby reduces the available surface water by 0.5% (Table 2). The increase in water consumption also increases the total volume of polluted water, thereby requiring more fresh water for dilution purposes. This positive feedback structure causes water-stress to rise roughly 7% in comparison to the baseline scenario. The considerable increase in agricultural land thus failed to produce a similar increase in food production.

The increase in water-stress generates an inverse impact on food production and ultimately poses negative impact on life expectancy. Table 2 shows a population change that can be judged insignificant with respect to the total population.

CO_2 emissions from fossil fuel and GDP are directly related to the population. The simulated results show very small changes for this scenario (see Table 2). However, the model results show a nearly 1% increase in global CO_2 concentration. This may be a significant finding. In reality, the atmospheric concentration of CO_2 does not originate solely in fossil fuel burning. A significant portion of carbon also comes from changes in land-use. In this simulation, the extra amount of atmospheric CO_2 concentration is the consequence of 15% increase in land conversion (specifically forest reduction) to expand the agricultural land.

A minor change in atmospheric CO_2 concentration contributes to a small increase in radiative forcing that affects the global temperature change. As the forcing from solar radiation and other gases remain unchanged, the effect of only 1% increase in CO_2 concentration dampens further. Since sea-level change is only a function of temperature, the model produces the same trend for the sea-level rise (see Table 2).

5.4. *High energy intensive scenario*

In the high energy intensive scenario the world is assumed to proceed towards higher dependency on carbon-intensive fossil fuel supported by higher rate of fossil fuel discovery. Under this scenario the technological development is considered as business as usual and the population growth rate is higher (compared to the base condition).

Increased population is not resulting in the significant increase of the global temperature. The only direct impact is seen in the increase of deforestation (conversion of forest land into agricultural land) to meet the growing food demand. Process of deforestation increases the rate of carbon release into the atmosphere and results in temperature change. However, the resulted radiative forcing is not high enough to increase the global temperature significantly.

The higher reserve of fossil fuel leads to a high carbon-intensive energy-based economy due to the lower fossil fuel price. Low fuel price prevents investment in clean fossil, renewable, and nuclear energy. Therefore, CO_2 emission from fossil fuel reaches its peak sharply until 2060 and then starts to decline due to the increase in fossil fuel price (the fuel price is inverse function of the stock, which starts decline rapidly during the fourth quarter of 21st century). So the cumulative effect of higher CO_2 production is increase in radiative forcing of close to 20%, triggering the global temperature increase of 0.70 °C compared to the base conditions (Fig. 8). It is expected that with this increase in temperature the sea level can raise up to 120 cm. Fig. 8 also shows that with this energy intensive scenario ANEMI_2 model results exhibit close resemblance with the IPCC A2 scenario (continuous population increase, regionally oriented economic development, and fragmented economic growth).

6. Discussion

Climate policy analyses can be well served by most of integrated assessment models. In order to effectively simulate climate policy, it is important that a model utilizes an optimization procedure and have an energy supply system component that takes into account the effects of non-renewable resource depletion. The ANEMI_2 model, presented in this paper, is developed to respond to these requirements. Other integrated assessment models have likewise utilized an optimization procedure and have incorporated an energy system component, including FREE (Fiddaman, 1997, 2002), TARGETS (Rotmans and de Vries, 1997), MESSAGE (Messner and Strubegger, 1995), and RICE (Nordhaus and Boyer, 2000). That provides for comparison of the ANEMI_2 model with other available models. The detailed results of model comparisons are out of the scope of this paper and are available in the publications by Akhtar (2011), and Akhtar et al. (2011).

The ANEMI model has been developed and implemented on the global scale for the study: "Analyzing Behaviour of the Society-Energy-Economy-Climate System" (Akhtar, 2011; Akhtar et al., 2011). As it combines a system dynamics-based simulation with a non-linear optimization procedure, it can be described as a computer-based system hybrid model. The model consists of nine system components (climate, carbon cycle, energy-economy, land-use, food production, population, hydrologic cycle, water demand, and water quality) with the time horizon extending up to 2085. It provides an inclusive portrait of availability of water resources, food production, population, emissions, global atmospheric temperature, and sea-level rise, as well as a detailed picture of energy demand and supply across several system components.

The model utilizes a one-period nonlinear optimization program for the energy–economy system component, while a part of this system component is going through the simulation process. Similar to the MESSAGE model (Messner and Strubegger, 1995), the ANEMI_2 optimization process is subject to constraints such as the availability of primary energy resources, the evolution of energy conversion technologies and a set of useful energy demands in different end-use system components. The model calculates an optimal and feasible energy supply-technology mix that requires the least total costs and meets a given useful or final energy demand.

Sensitivity of the system component parameters of the ANEMI model is tested while setting up and calibrating the individual system components even though they are mostly based on the well-understood and well-established quantifiable elements of the global system (Davies, 2007; Davies and Simonovic, 2008, 2010). A simplified sensitivity analysis has been performed by fully integrated version of the ANEMI (ANEMI_2) model presented in this paper. Some parameters (such as reproductive lifetime) are found to be more sensitive than others like: average lifetime of the land, technological development delay, etc. Therefore, the targeted uncertainty analyses helps to visualize the robustness of the ANEMI_2 model in the presence of uncertainty and at the same time can increase our understanding of the relationships between input and output variables of the model.

A good climate policy demands the best possible understanding of climate change and its subsequent impact on human life. While it is almost impossible to find or develop a model that is capable of providing everything accurately, an integrated assessment model must be able to provide credible output. The ANEMI_2 model is designed to provide accurate and credible results concerning the long-term impacts of various policy options on the society-energy-economy-climate system. In the presented results, three policy scenarios are used to illustrate model use and investigate model utility in climate policy development. These policy scenarios respond to real concerns of participating policy makers, even though they do not include the real data and the policy implementation timeframe.

Under the carbon tax policy a carbon tax is implemented in 2012 and slowly ramped up to $100 per tonne of CO_2 emissions

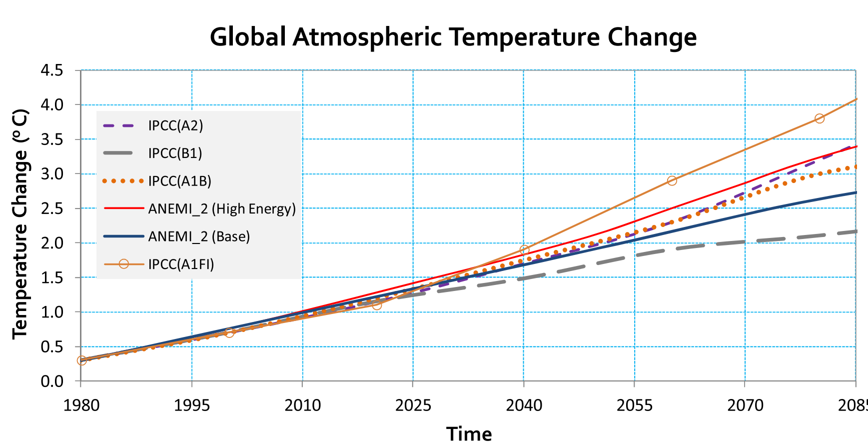

Fig. 8. Global Atmospheric Temperature Comparison.

over the next 30 years. The model results show a considerable influence on energy production as the initial consumption declines, so the reserves decline more slowly, ensuring more reserves in the future. Such decline also lowers the fossil fuel based CO_2 emissions, as it does the atmospheric temperature. Since temperature is a directly related factor in sea-level rise, the latter also shows a lower value. These favorable changes result in a more environmentally friendly situation that subsequently invites an increase in population and thus more demand for food and water. To meet this growing demand, more land area is required to be converted into irrigated area. This leads to increased pressure on available water resources with respect to water quantity and quality, which can be defined as water-stress. Increased water-stress works as a negative feedback for further growth and leads to a more stable global conditions.

A 15% increase in water consumption is introduced under the water use increase scenario to meet the growing water demand related to climate change. Such an increase in consumption lowers the available surface water, resulting in 6% increase in water-stress. The most affected system component in this case is agriculture which shows loss of more than 5% of its regular production. An increase in water-stress and a decrease in food production together exhibit threat to average human life expectancy. The population is thus expected to drop by 7.5%. The GDP likewise drops, but only nominally. With the reduced population, CO_2 production from the burning of fossil fuel decreases. However, there is little noticeable change in the atmospheric temperature, since the reduced amount of CO_2 from the atmosphere is insignificant compared to total GHGs equivalent.

Food production increase scenario tests the impact of redistributing land-use, by converting 15% land from forest to agriculture. The simulation results show that this expansion of agricultural land is not able to increase food production in the long run. Rather, total food production declines on the global scale. Both, the extra irrigation demands from the newly converted land and the increased population (at the initial stage) create great pressure on the scarce water resources, increasing the water-stress beyond the tolerable range. Such a stressful condition hampers food production, human life expectancy, and so on. As the population declines, CO_2 emissions continue to increase due to land conversion (forest cutting/burning). Still, such an increase in CO_2 emissions is not able to increase the radiative forcing noticeably. So the atmospheric temperature and sea-level rise remain almost unchanged.

High energy intensive scenario, with the world with higher dependency on carbon-intensive fossil fuel shows that CO_2 emissions reach their peak sharply by 2060. Later on the CO_2 emissions stay almost steady for a while and then start to decline because of increased fossil fuel price associated with diminishing fossil fuel reserves. Such an increase in CO_2 production amplifies the radiative forcing by close to 20%, triggering the global temperature increase of 0.70 °C above the base condition. The simulated results from this scenario exhibit close resemblance with the IPCC A2 scenario.

Several of the ANEMI_2 model system components are built from the basic structure of the ANEMI_1 model (Davies and Simonovic, 2009). However, they are integrated in a novel way, particularly the water system components. The integration of optimization within the simulation framework of the ANEMI_2 model is timely, as recognition grows of the importance of energy-based economic activities in determining long-term Earth-system behavior. Experimentation with different policy scenarios demonstrates the consequences of these activities on future behavior of the society-biosphere-climate-economy-energy system through feedback based interactions. The use of the ANEMI_2 model improves both scientific understanding and socio-economic policy development strategy.

7. Future work

Integrated assessment modeling has the unique ability to unite the natural and social sciences. In the last twenty years, it has developed into an increasingly important tool for climate change research. The current energy-economy sector of the ANEMI_2 model may require some further improvements. At this stage of model development, the approach taken in the modeling of electric energy production is myopic, as the simulated investment decisions do not consider the future of the process. Moreover, the model tends to break down when the total cost of electricity production from the fossil fuel rises exponentially, due to the inability of capital stock to adjust optimally. The inclusion of the optimal capital stock adjustment mechanism in combination with the forward looking behavior is the first future research step in the development of a more robust energy-economy sector of the ANEMI_2 model. The introduction of a 'back-stop' technology (Kemfert, 2000), where at a threshold price a greenhouse gas free energy source could become more cost-effective, is being considered.

The land-use sector of the current version of the ANEMI_2 model requires further improvement. The aggregate description of land-use change remains insufficient for better understanding of the regional/local land-use related processes. Experimentation with different drivers, including population, economic output, and climatic effects is in progress to assist in finding the links with the possible land-use change patterns. An improvement in the understanding of both, the causes and the effects of the land-use change at the global scale should therefore make the model results of more value at different spatial scales.

It is recommended that future model expansion consider addition of the animal sub-component under Food Production system component.

Water is the most valuable global resource. It is necessary for human survival, and it thus determines the overall prospects of a country. Unfortunately, such an important resource is not abundant all over the world – many areas are under water-stress conditions. Therefore, water conservation is no longer an efficient option for solving the crisis. Anything scarce and in demand commands a price; this is one of the basic principles of economics. Two particular areas of water policy that are becoming increasingly subject to pricing principles are those of public water supply and waste water services. Water sectors in the ANEMI_2 model are not yet linked with the economy sector. Therefore, an investigation of water pricing scenarios endogenously is not yet possible. The future implementation of the market clearing mechanism for the water sectors will therefore definitely guide the model along the path of environmental sustainability.

We have implemented the ANEMI_2 to investigate a limited number of policy scenarios derived through the discussions among a narrow group of participating decision makers. But while this current group of partners have provided important insights, further expansion of model implementation scenarios is under consideration. Many important questions raised in the course of this research will be addressed with future model modification. Our intention is to continue work with expanded group of partners that will include different government departments. In addition, further research on the international climate change related policy will be an important input for the future model simulations required for the assessment of global consequences.

Acknowledgments

We are grateful to the Natural Sciences and Engineering Research Council of Canada (NSERC) for its support to Professor

Slobodan P. Simonovic and his collaborators, through the Strategic Research Grant, which funded development of the ANEMI_2 model.

References

Akhtar, M.K., 2011. A System Dynamics Based Integrated Assessment Modelling of Global-Regional Climate Change: a Model for Analyzing the Behaviour of the Social-Energy-Economy-Climate System. Electronic Thesis and Dissertation Repository. Paper 331.

Akhtar, M.K., Simonovic, S.P., Wibe, J., MacGee, J., Davies, J., 2011. An Integrated System Dynamics Model for Analyzing Behaviour of the Social-Energy-Economy-Climate System: User's Manual. Water Resources Research Report no. 076. Facility for Intelligent Decision Support, Department of Civil and Environmental Engineering, London, Ontario, Canada, p. 161. ISBN: (print) 978-0-7714-2897-5; (online) 978-0-7714-2904-0.

Alcamo, J., 1994. Preface. Water, Air, & Soil Pollution 76, 1–2.

Alcamo, J., Henrichs, T., 2002. Critical regions: a model-based estimation of world water resources sensitive to global changes. Aquatic Sciences 64, 352–362.

Alcomo, J., Döll, P., Henrichs, T., Kaspar, F., Lehner, B., Rösch, T., Siebert, S., 2003. Development and testing of the WaterGAP 2 global model of water use and availability. Hydrological Sciences Journal 48 (3), 317–337.

Almeder, C., Margaretha, P., 2007. A hybrid simulation optimization approach for supply chains-multimethod simulation software tool AnyLogic. In: EUROSIM 2007, Ljubljana, Slovenia.

Amodeo, L., Prins, C., Sánchezin, D.R., 2009. Comparison of Metaheuristic Approaches for multi-objective simulation-based optimization in supply chain inventory management. Applications of evolutionary computing EvoWorkshops 2009. Lecture Notes in Computer Science 5484, 798–807.

Applegate, W.B., Runyan, J.W., Brasfield, L., Williams, M.L., Konigsberg, C., Fouche, C., 1981. Analysis of the 1980 heat wave in Memphis. Journal of the American Geriatrics Society 29 (8), 337–342.

AQUASTAT, 2010. FAO's Information System on Water and Agriculture. Food and Agriculture Organization of the Unites Nations. Available from: http://www.fao.org/nr/water/aquastat/main/index.stm (last accessed 12.12.10.).

Azadivar, F., Truong, T., Stokesbury, K.D.E., Rothschild, B.J., 2002. Simulation based optimization in fishery management. In: Proceedings of the 2002 Winter Simulation Conference. Citeseer.

Ballester, F., Corella, D., Perez-Hoyos, S., Saez, M., Hervas, A., 1997. Mortality as a function of temperature: a study in Valencia, Spain, 1991–1993. International Journal of Epidemiology 26, 551–561.

Bashi-Azghadi, S.N., Kerachian, R., 2010. Locating monitoring wells in groundwater systems using embedded optimization and simulation models. Science of the Total Environment 408 (10), 2189–2198.

Basu, R., 2009. High ambient temperature and mortality: a review of epidemiologic studies from 2001 to 2008. Environmental Health 8, 40. http://dx.doi.org/10.1186/1476-069X-8-40.

Basu, R., Ostro, B.D., 2008. A multicounty analysis identifying the populations vulnerable to mortality associated with high ambient temperature in California. American Journal of Epidemiology 168, 632–637.

Basu, R., Samet, J.M., 2002. Relation between elevated ambient temperature and mortality: a review of the epidemiologic evidence. Epidemiologic Reviews 24, 190–202.

Climate change and water. In: Bates, B.C., Kundzewicz, Z.W., Wu, S., Palutikof, J.P. (Eds.), Technical Paper VI of the Intergovernmental Panel on Climate Change. IPCC Secretariat, Geneva, p. 210.

Bhattacharjya, R.K., Datta, B., 2005. Optimal management of coastal aquifers using linked simulation optimization approach. Water Resources Management 19 (3), 295–320.

Bland, W.L., 1990. Toward integrated assessment in agriculture. Agricultural Systems 60, 157–167.

Bruinsma, J., 2009. The resource outlook to 2050: by how much do land, water and crop yields need to increase by 2050?. In: Paper Presented at the FAO Expert Meeting on How to Feed the World in 2050, 24–26 June 2009, Rome.

Calvin, K., Edmonds, J., Bond-Lamberty, B., Clarke, L., Kim, S.H., Kyle, P., Smith, S.J., Thomson, A., Wise, M., 2009. 2.6: limiting climate change to 450 ppm CO2 equivalent in the 21st century. Energy Economics 31 (Supplement Suppl. 2), S107–S120.

Carnevale, C., Finzi, G., Pisoni, E., Volta, M., Guariso, G., Gianfreda, R., Maffeis, G., Thunis, P., White, L., Triacchini, G., 2012. An integrated assessment tool to define effective air quality policies at regional scale. Environmental Modelling & Software 38, 306–315.

Cetinkaya, C.P., Fistikoglu, O., Fedra, K., Harmancioglu, N.B., 2008. Optimization methods applied for sustainable management of water-scarce basins. Journal of Hydroinformatics 10, 69–95.

Chapagain, A.K., Hoekstra, A.Y., Savenije, H.H.G., Gautam, R., 2006. The water footprint of cotton consumption: an assessment of the impact of worldwide consumption of cotton products on the water resources in the cotton producing countries. Ecological Economics 60 (1), 186–203.

Church, J.A., White, N.J., 2006. A 20th century acceleration in global sea-level rise. Geophysical Research Letters 33, L01602. http://dx.doi.org/10.1029/2005GL024826.

Conn, A.R., Gould, N.I.M., Toint, P.L., 2000. Trust-region Methods. SIAM Publications, Philadelphia, Pennsylvania.

Dabrowski, J.M., Murray, K., Ashton, P.J., Leaner, J.J., 2009. Agricultural impacts on water quality and implications for virtual water trading decisions. Ecological Economics 68, 1074–1082.

Davies, E.G.R., 2007. Modelling Feedback in the Society-Biosphere-Climate System. Ph.D. thesis. Department of Civil and Environmental Engineering, the University of Western Ontario, London, Ontario, Canada.

Davies, E.G.R., Simonovic, S.P., 2008. An Integrated System Dynamics Model for Analyzing Behaviour of the Social-Economic-Climatic System: Model Description and Model Use Guide. Water Resources Research Report no. 059, Facility for Intelligent Decision Support. Department of Civil and Environmental Engineering, London, Ontario, Canada, p. 233. ISBN: (print) 978-0-7714-2679-7; (online) 978-0-7714-2680-3.

Davies, E.G.R., Simonovic, S.P., 2009. Energy Sector for the Integrated System Dynamics Model for Analyzing Behaviour of the Social-Economic-Climatic Model. Water Resources Research Report no. 063, Facility for Intelligent Decision Support. Department of Civil and Environmental Engineering, London, Ontario, Canada, p. 191. ISBN: (print) 978-0-7714-2712-1; (online) 978-0-7714-2713-8.

Davies, Evan G.R., Simonovic, S.P., 2010. ANEMI: a new model for integrated assessment of global change. Interdisciplinary Environmental Review 11 (2/3), 127–161.

Davies, E.G.R., Simonovic, S.P., 2011. Global water resources modeling with an integrated model of the social-economic-environmental system. Advances in Water Resources 34 (6), 684–700.

Diaz, J., Linares, C., Tobias, A., 2006. Impact of extreme temperatures on daily mortality in Madrid (Spain) among the 45–64 age-group. International Journal of Biometeorology 50, 342–348.

Dowlatabadi, H., 2000. Bumping against a gas ceiling. Climatic Change 46 (3), 391–407.

Dowsett, H., Thompson, R., Barron, J., Cronin, T., Fleming, F., Ishman, S., Poore, R., Willard, D., Holtz Jr., T., 1994. Joint investigations of the Middle Pliocene climate I: PRISM paleoenvironmental reconstructions. Global and Planetary Change 9 (3–-4), 169–195.

Ellis, F.P., Nelson, F., 1978. Mortality in the elderly in a heat wave in New York City, August 1975. Environmental Research 15, 504–512.

Ellis, F.P., Prince, H.P., Lovatt, G., Whittington, R.M., 1980. Mortality and morbidity in Birmingham during the 1976 heat wave. Quarterly Journal of Medicine 49, 1–8.

El-Zein, Abbas, Mylene, T., 2005. On the association between high temperature and mortality in warm climates. Science of the Total Environment 343 (1), 273–275.

Erdem, A.S., Sancarin, U.A., 2006. A simulation based DSS design for supply chain management. In: Technology Management for the Global Future PICMET 2006 Conference, vol. 6(c), pp. 2741–2747.

Ewert, F., Van Ittersum, M.K., Bezlepkina, I., Therond, O., Andersen, E., Heckelei, T., et al., 2009. A methodology for enhanced flexibility of integrated assessment in agriculture. Environmental Science & Policy 12, 546–561.

FAO, 2009. Global Agriculture towards 2050, High Level Expert Forum – How to Feed the World in 2050 Office of the Director. Agricultural Development Economics Division Economic and Social Development Department, Rome, Italy. Available from: http://www.fao.org/fileadmin/templates/wsfs/docs/Issues_papers/HLEF2050_Global_Agriculture.pdf (last accessed 30.05.11.).

Fedra, K., Harmancioglu, N.B., 2005. A web-based water resources simulation and optimisation system. In: Savic, D., Walters, G., King, R., Khu, A.-T. (Eds.), Proc. of CCWI 2005 on Water Management for the 21st Century, vol. 2. Center of Water Systems, Univ. of Exeter, pp. 167–172.

Fiddaman, T.S., 1997. Feedback Complexity in Integrated Climate-Economy Models. Ph.D. thesis. Alfred P. Sloan School of Management, Massachusetts Institute of Technology, Boston, Massachusetts, U.S.A.

Fiddaman, T.S., 2002. Exploring policy options with a behavioral climate-economy model. System Dynamics Review 18, 243–267.

Forrester, J.W., 1958. Industrial dynamics: a major breakthrough for decision makers. Harvard Business Review 36, 37–66.

Gouveia, N., Hajat, S., Armstrong, B., 2003. Socioeconomic differentials in the temperature-mortality relationship in Sao Paulo, Brazil. International Journal of Epidemiology 32, 390–397.

Harvey, L.D.D., Schneider, S.H., 1985. Transient climate response to external forcing on 10^0–10^4 year time scales. Part I: experiments with globally averaged, coupled, atmosphere and ocean energy balance models. Journal of Geophysical Research 90 (D1), 2191–2205.

Hung, W.Y., Kucherenko, S., Samsatli, N.J., Shah, N., 2004. A flexible and generic approach to dynamic modeling of supply chains. Journal of the Operations Research Society 55, 801–813.

Intergovernmental Panel on Climate Change (IPCC), 2007a. Climate change 2007: the physical science basis. In: Solomon, S., Qin, D., Manning, M., Chen, Z., Marquis, M., Averyt, K.B., Tignor, M., Miller, H.L. (Eds.), Contribution of Working Group I to the Fourth Assessment Report of the Intergovernmental Panel on Climate Change. Cambridge University Press, Cambridge, United Kingdom and New York, NY, USA, p. 996.

Intergovernmental Panel on Climate Change (IPCC), 2007b. Summary for policymakers. In: Parry, M.L., Canziani, O.F., Palutikof, J.P., van der Linden, P.J., Hanson, C.E. (Eds.), Climate Change 2007: Impacts, Adaptation and Vulnerability, Contribution of Working Group II to the Fourth Assessment Report of the Intergovernmental Panel on Climate Change. Cambridge University Press, Cambridge, UK, pp. 7–22.

Intergovernmental Panel on Climate Change (IPCC), 2007c. Climate change 2007: synthesis report. In: Core Writing Team, Pachauri, R.K., Reisinger, A. (Eds.),

Contribution of Working Groups I, II and III to the Fourth Assessment Report of the Intergovernmental Panel on Climate Change. IPCC, Geneva, Switzerland, p. 104.
Jacobson, M., Charlson, R.J., Rodhe, H., Orians, G.H., 2008. Earth System Science – from Biogeochemical Cycles to Global Change. Elsevier, Amsterdam.
Jevrejeva, S., Moore, J.C., Grinsted, A., 2010. How will sea level respond to changes in natural and anthropogenic forcings by 2100? Geophysical Research Letters 37, L07703 http://dx.doi.org/10.1029/2010GL042947.
Jones, T.S., Liang, A.P., Kilbourne, E.M., Griffin, M.R., Patriarca, P.A., Wassilak, S.G., Mullan, R.J., Herrick, R.F., Donnell, H.D., Choi, K., Thacker, S.B., 1992. Morbidity and mortality associated with the July 1980 heat wave in St Louis and Kansas City. Mo. Journal of the American Medical Association 247, 3327–3331.
Kasperska, E., Slota, D., 2003. Two different methods of embedding the optimization in simulation on model DYNBALANCE(2–2). In: Davidsen, P.I., Mollona, E. (Eds.), Proc. 21 International Conference of the System Dynamics Society. SDS, New York.
Kasperska, E., Mateja-Losa, E., Slota, D., 2000. Some extension of system dynamics method – theoretical aspects. In: Deville, M., Owens, R. (Eds.), Proc. 16th IMACS World Congress. IMACS, Lausanne.
Kasperska, E., Mateja-Losa, E., Slota, D., 2001. Some dynamics balance of production via optimization and simulation within system dynamics method. In: Hines, J.H., Diker, V.G., Langer, R.S., Rowe, J.I. (Eds.), Proc. 19th International Conference of the System Dynamics Society. SDS, Atlanta, pp. 1–18.
Kearney, J., 2010. Food consumption trends and drivers. Philosophical Transactions of the Royal Society B. 365, 2793–2807.
Kelly, R.A., Jakeman, A.J., Barreteau, O., Borsuk, M.E., ElSawah, S., Hamilton, S.H., Henriksen, H.J., Kuikka, S., Maier, H.R., Rizzoli, A.E., van Delden, H., Voinov, A.A., 2013. Selecting among five common modelling approaches for integrated environmental assessment and management. Environmental Modelling & Software 47, 159–181.
Kemfert, C., 2000. An integrated assessment model of economy-energy-climate – the model Wiagem. Integrated Assessment 3 (4), 281–298.
Kundzewicz, Z.W., Mata, L.J., Arnell, N.W., Döll, P., Kabat, P., Jiménez, B., Miller, K.A., Oki, T., Sen, Z., Shiklomanov, I.A., 2007. Freshwater resources and their management. Climate change 2007: impacts, adaptation and vulnerability. In: Parry, M.L., Canziani, O.F., Palutikof, J.P., van der Linden, P.J., Hanson, C.E. (Eds.), Contribution of Working Group II to the Fourth Assessment Report of the Intergovernmental Panel on Climate Change. Cambridge University Press, Cambridge, UK, pp. 173–210.
Kunzig, R., 2009. The Big Idea. National Geographic. Edited: December 2009, (last accessed 27.01.10.) http://ngm.nationalgeographic.com/big-idea/05/carbon-bath.
Laniak, G.F., Rizzoli, A.E., Voinov, A., 2013. Thematic issue on the future of integrated modeling science and technology. Environmental Modelling & Software 39 (Special Issue), 1–330.
Law, A.M., McComas, M.G., 2000. Simulation-based optimization. In: Proceedings of the 2000 Winter Simulation Conference. Orlando, USA.
Leimbach, M., Bauer, N., Baumstark, L., Lüken, M., Edenhofer, O., 2010. Technological change and international trade – insights from REMIND-R. Energy Journal 31 (Special Issue), 109–136.
Lehtonen, H.S., Rotter, R.P., Palosuo, T.I., Salo, T.J., Helin, J.A., Pavlova, Y., Kahiluoto, H.M., 2010. A modeling framework for assessing adaptive management options of Finnish agrifood systems to climate change. Journal of Agricultural Science 2 (2), 3–16.
Luderer, G., Bosetti, V., Steckel, J., Waisman, H., Bauer, N., Decian, E., Leimbach, M., Sassi, O., Tavoni, M., 2009. The Economics of Decarbonization – Results from the RECIPE Model Intercomparison. Available online at: http://www.pik-potsdam.de/recipe (last accesses23.09.11.).
Macfarlane, A., 1978. Daily mortality and environment in English conurbations. II. Deaths during summer hot spells in Greater London. Environmental Research 15, 332–341.
Manne, A.S., Mendelsohn, R., Richels, R., 1995. MERGE – a model for evaluating regional and global effects of GHG reduction policies. Energy Policy 23 (1), 17–34.
Martens, W.J.M., 1998. Climate change, thermal stress and mortality changes. Social Science & Medicine 46 (3), 331–344.
Matsuoka, Y., Kainuma, M., Morita, T., 1995. Scenario analysis of global warming using the Asian-Pacific Integrated Model (AIM). Energy Policy 23 (4–5), 357–371.
McKinney, D., Savitsky, A., 2003. Basic Optimization Models for Water and Energy Management. Prepared under USAID Contract No. Washington D.C.
Meadows, Dennis L., Behrens, William W., Meadows, Donella H., Naill, Roger F., Randers, Jorgen, Zahn, Erich K.O., 1974. Dynamics of Growth in a Finite World. Wright-Allen Press, Inc, Cambrigde, Massachusetts.
Meadows, Donella H., Meadows, D.L., Rendersm, J., 1992. Beyond the Limits: Confronting Global Collapse Envisioning a Sustainable Future. Chelsea Green Publishing Company, New York.
Meadows, D.H., Randers, J., Meadows, D., 2004. Limits to Growth: the Thirty Year Update. Chelsea Green Publishing Company, White River Junction, Vermont, United States.
Meinshausen, M., Raper, S.C.B., Wigley, T.M.L., 2008. Emulating IPCC AR4 atmosphere-ocean and carbon cycle models for projecting global-mean, hemispheric and land/ocean temperatures: MAGICC 6.0. Atmospheric Chemistry & Physics Discussion 8, 6153–6272.
Messner, S., Strubegger, M., 1995. User's Guide for MESSAGE III, WP-95-69. International Institute for Applied Systems Analysis, Laxenburg, Austria.
Neilsen, D., Smith, S., Koch, W., Frank, G., Hall, J., Parchomchuk, P., 2001. Impact of Climate Change on Crop Water Demand and Crop Suitability in the Okanagan Valley, British Columbia. Technical Bulletin 01-15. Pacific Agri-Food Research Centre, Summerland, BC, p. 32. Available: from http://www.obwb.ca/obwrid/docs/005_2001_Climate_Change_on_Crop_Water.pdf (last accessed 30.07.11.).
Nichollas, N., 2009. Estimating changes in mortality due to climate change. Climate Change 97, 313–320.
Nordhaus, W.D., 1994. Managing the Global Commons: the Economics of Climate Change. MIT Press, Cambridge, Mass.
Nordhaus, W.D., 2007. Accompanying Notes and Documentation on Development of DICE-2007 Model. Yale University.
Nordhaus, W.D., 2008. A Question of Balance: Weighing the Options on Global Warming Policies. Yale University Press, New Haven, CT.
Nordhaus, W.D., Boyer, J., 2000. Warming the World: Economic Models of Global Warming. The MIT Press, Cambridge, Massachusetts, U.S.A.
Nordhaus, W.D., Yang, Z., 1996. A regional dynamic general-equilibrium model of alternative climate-change strategies. The American Economic Review 86 (4), 741–765.
O'Neill, M.S., Hajat, S., Zanobetti, A., Ramirez-Aguilar, M., Schwartz, J., 2005. Impact of control for air pollution and respiratory epidemics on the estimated associations of temperature and daily mortality. International Journal of Biometeorology 50, 121–129.
Overpeck, J.T., Weiss, J.L., 2009. Projections of future sea level becoming dire. Proceeding of the National Academy of Science of the United States of America 106 (51), 21461–21462.
Parson, E.A., 1994. Searching for integrated assessment: a preliminary investigation of methods and projects in the integrated assessment of global climatic change. In: Paper Presented to the Third Meeting of the Harvard-ciesin Commission on Global Environmental Change Information Policy. NASA Headquarters, Washington, DC.
Popovich, C.J., Simonovic, S.P., McBean, G.A., 2010. Use of an Integrated System Dynamics Model for Analyzing Behaviour of the Social-economic-climatic System in Policy Development. Water Resources Research Report no. 067, Facility for Intelligent Decision Support. Department of Civil and Environmental Engineering, The University of Western Ontario, p. 37. ISBN: (print) 978-0-7714-2838-8; (online) 978-0-7714-2839-5.
Postel, S., 1999. Pillar of Sand – Can the Irrigation Miracle Last? Norton W. W. & Company, New York, USA, p. 312.
Prinn, R., Jacoby, H., Sokolov, A., Wang, C., Xiao, X., Yang, Z., Eckhaus, R., Stone, P., Ellerman, D., Melillo, J., Fitzmaurice, J., Kicklighter, D., Holian, G., Liu, Y., 1999. Integrated global system model for climate policy assessment: feedbacks and sensitivity studies. Climatic Change 41 (3–4), 469–546.
Pulido-Velazquez, M., Andreu, J., Sahuquillo, A., 2006. Economic optimization of conjunctive use of surface water and groundwater at the basin scale. Journal of Water Resources Planning and Management 132 (6), 454–546.
Rahmstorf, S., 2007. A semi-empirical approach to projecting future sea-level rise. Science 315, 368–370.
Rost, S., Gerten, D., Bondeau, A., Luncht, W., Rohwer, J., Schaphoff, S., 2008. Agricultural green and blue water consumption and its influence on the global water system. Water Resources Research 44, W09405. http://dx.doi.org/10.1029/2007WR006331.
Rotmans, J., 1990. IMAGE: an Integrated Model to Assess the Greenhouse Effect. Kluwer Academic Publishers, Dordrecht, the Netherlands.
Rotmans, J., de Vries, B., 1997. Perspectives on Global Change: the Targets Approach. Cambridge Univ. Pres, Cambridge.
Rotmans, J., van Asselt, M.B.A., de Vries, B.J.M., Beusen, A.H.W., den Elzen, M.G.J., Hilderink, H.B.M., Hoekstra, A.Y., Janssen, M.A., Köster, H.W., Niessen, L.W., Strengers, B.J., 1997b. The TARGETS model. In: Rotmans, J., de Vries, B. (Eds.), Perspectives on Global Change: the TARGETS Approach. Cambridge University Press, Cambridge, U.K, pp. 33–54.
Saez, M., Sunyer, J., Castellsague, J., Murillo, C., Anto, J.M., 1995. Relationship between weather temperature and mortality: a time series analysis approach in Barcelona. International Journal of Epidemiology 24 (3), 576–582.
Safavi, H.R., Darzi, F., Mariño, M.A., 2010. Simulation-optimization modeling of conjunctive use of surface water and groundwater. Water Resources Management 24 (10), 1965–1988.
Schneider, S., Sarukhan, J., Adejuwon, J., Azar, C., Baethgen, W., Hope, C., Moss, R., Leary, N., Richels, R., van Ypersele, J.P., 2001. Overview of impacts, adaptation, and vulnerability to climate change. In: Climate Change 2001: Impacts, Adaptation and Vulnerability. Contribution of Working Group II to the Third Assessment Report of the Intergovernmental Panel on Climate Change. Cambridge University Press, Cambridge, United Kingdom and New York, NY, USA.
Shafer, W., Sonnenschein, H., 1975. Equilibrium in abstract economies without ordered preferences. Journal of Mathematical Economics 2 (3), 345–348.
Simonovic, S.P., 2009. Managing Water Resources: Methods and Tools for a Systems Approach. UNESCO Publishing, Paris.
Singh, R., 2011. Design of barrages with genetic algorithm based embedded simulation optimization approach. Water Resources Management 25 (2), 409–429.
Smoyer-Tomic, K.E., Rainham, D.G., 2001. Beating the heat: development and evaluation of a Canadian hot weather health-response plan. Environ Health Perspect 109, 1241–1248.
Stanley, J., 2009. Hill Country Landowner's Guide. Texas A&M University Press, College Station.
Sterman, J.D., 2000. Business Dynamics. Systems Thinking and Modeling for a Complex World. Irwin McGraw- Hill, Boston, MA.

Trenberth, K.E., Jones, P.D., Ambenje, P., Bojariu, R., Easterling, D., Klein Tank, A., Parker, D., Rahimzadeh, F., Renwick, J.A., Rusticucci, M., Soden, B., Zhai, P., 2007. Observations: surface and atmospheric climate change. In: Solomon, S., Qin, D., Manning, M., Chen, Z., Marquis, M., Averyt, K.B., Tignor, M., Miller, H.L. (Eds.), Climate Change 2007: the Physical Science Basis, Contribution of Working Group I to the Fourth Assessment Report of the Intergovernmental Panel on Climate Change. Cambridge University Press, Cambridge, United Kingdom and New York, NY, USA.

Tol, R.S.J., Fankhauser, S., 1998. On the representation of impact in integrated assessment models of climate change. Environmental Modeling & Assessment 3, 63–74.

Truong, T.H., Azadivar, F., 2003. Simulation based optimization for supply chain configuration design. In: WSC '03 Proceedings of the 35th Conference on Winter Simulation: Driving Innovation, vol. 2, pp. 1268–1275.

Van Ittersum, M.K., Ewert, F., Heckelei, T., Wery, J., Alkan Olsson, J., et al., 2008. Integrated assessment of agricultural systems – a component-based framework for the European Union (SEAMLESS). Agricultural Systems 96, 150–165.

Van Vuuren, D.P., Eickhout, B., Lucas, P.L., den Elzen, M.G.J., 2006. Long-term multi-gas scenarios to stabilise radiative forcing – exploring costs and benefits within an integrated assessment framework. Energy Journal 27 (Special Issue: 3), 201–233.

Ventana Systems, 2010. Vensim Reference Manual (On Line). Ventana Systems, Inc, Harvard, Massachusetts, U. S. A. Available: from http://www.vensim.com/documentation.html (last accessed 12.01.11.).

Vermeer, M., Rahmstorf, S., 2009. Global sea level linked to global temperature. Proceeding of the National Academy of Science of the United States of America 106 (51), 21527.

Von Deimling, T.S., Ganopolski, A., Held, H., Rahmstorf, S., 2006. How cold was the last glacial maximum? Geophysical Research Letters 33, L14709 http://dx.doi.org/10.1029/2006GL026484.

Waelbroeck, C., Labeyrie, L., Michel, E., Duplessy, J.C., McManus, J.F., Lambeck, K., Balbon, E., Labracherie, M., 2002. Sea-level and deep water temperature changes derived from benthic foraminifera isotopic records. Quaternary Science Reviews 21, 295–305.

Wainwright, S.H., Buchanan, S.D., Mainzer, M., Parrish, R.G., Sinks, T.H., 1999. Cardiovascular mortality—the hidden peril of heat waves. Prehospital and Disaster Medicine 14, 222–231.

Watson, D.J., van Binsbergen, J., 2008. Livestock Market Access and Opportunities in Turkana, Kenya. ILRI Research Report 3. ILRI (International Livestock Research Institute), Nairobi, Kenya, p. 106.

Weyant, J., Davidson, O., Dowlatabadi, H., Edmonds, J., Grubb, M., Richels, R., Rotmans, J., Shukla, P., Cline, W., Fankhauser, S., Tol, R., 1996. Integrated assessment of climate change: an overview and comparison of approaches and results. In: Bruce, J.P., Lee, H., Haites, E.F. (Eds.), Climate Change 1995–economic and Social Dimensions of Climate Change, Contribution of Working Group III to the Second Assessment Report of the Intergovernmental Panel on Climate Change (IPCC). Cambridge University Press, Cambridge.

Weyant, J.P., 1994. Integrated assessment of climate change: a overview and comparison of modeling approaches. In: Paper for the Writing Team 6/7 of Working III Intergovernmental Panel on Climate Change Lead Authors Meeting, Geneva.

Winz, I., Brierley, G., Trowsdale, S., 2009. The use of system dynamics simulation in water resources management. Water Resources Management 23, 1301–1323.